MINIMIZING TRANSIENTS VIA THE KREISS SYSTEM NORM

PIERRE APKARIAN[1] AND DOMINIKUS NOLL[2]

ABSTRACT. We consider norms which assess transient behavior of stable LTI systems. Minimizing such a norm in closed loop may enhance stability and performance of a nonlinear system by mitigating transients and enlarging its region of attraction around a locally stable steady state.

KEY WORDS. transient mitigation, L_1 disturbance, Kreiss constant, structured controller, suppression of attractors, non-smooth optimization, LMI design techniques.

1. INTRODUCTION

It has been observed in the literature that the size of the region of attraction of a locally stable nonlinear system

$$\dot{x} = Ax + \phi(x), \quad x(0) = x_0 \tag{1}$$

with $\phi(0) = 0$, $\phi'(0) = 0$, may strongly depend on the degree of normality of A. When A is far from normal, the linearization $\dot{x} = Ax$, $x(0) = x_0$, may have large transient peaks, which may incite trajectories of (1) to leave the region of attraction. This is known as *peaking*, [43, 29, 19], and considered a major obstacle to global stability.

The tendency of a stable A to produce large transients or peaking may be assessed by its worst-case transient growth

$$M_0(A) = \max_{t\geq 0} \max_{\|x_0\|_2=1} \|e^{At}x_0\|_2 = \max_{t\geq 0} \overline{\sigma}(e^{At}), \tag{2}$$

and in closed loop, when A depends on tunable parameters, one may attempt to minimize $M_0(A_{\rm cl})$ in order to enlarge the region of local stability of (1). This has been studied in [8] for structured controllers, and previously in [21] using the controller Q-parametrization.

The rationale underlying this approach should be further deepened by taking two more facts into account. Firstly, in a continuous operating process the effect of initial values is not the appropriate lever, as instability is rather caused by noise, persistent perturbations, or finite-consumption disturbances. Secondly, nonlinearity often arises only in some of the states z, and likewise may affect only parts of the dynamics, and the heuristic should be adaptable to such cases. We address those issues by considering a nonlinear controlled system of the form

$$\begin{aligned} \dot{x} &= Ax + B\phi(z) + Bw + B_u u \\ z &= Cx \\ y &= C_y x \end{aligned} \tag{3}$$

where the nonlinearity satisfies $B\phi(0) = 0$ and $B\phi'(0)C = 0$, and where a tunable feedback controller $u = K(\mathbf{x})y$, with $\mathbf{x}$ as decision variables, is sought which stabilizes the system locally, rendering it as resilient as possible with regard to these disturbances. The latter is aimed at indirectly by tuning the closed loop channel $w \to z$ to remain small with regard to a system norm assessing transients, the idea being that disturbances w cause the partial state z to have unduly large transients.

[1]ONERA, Department of System Dynamics, Toulouse, France.
[2]Institut de Mathématiques, Université de Toulouse, France.

More formally, we close the loop with respect to the controller $K(\mathbf{x})$ in (3), and consider the linear closed-loop channel $T_{wz}(\mathbf{x}, s) = C(sI - A_{\rm cl}(\mathbf{x}))^{-1}B$, which we now tune in such a way that transients in $z(t)$ due to disturbances $w(t)$ remain small. Expanding on (2), we may assess transients of $G(s) = C(sI - A)^{-1}B$ via

$$\mathcal{M}_0(G) = \sup_{t\geq 0} \overline{\sigma}\left(Ce^{At}B\right) = \sup_{\|w\|_1\leq 1} \|G * w\|_\infty, \tag{4}$$

which turns out to be a time-domain $L^1 \to L^\infty$ induced system norm with suitably chosen vector norms. It measures the time-domain peak of the response $z = G * w$ of G to a finite consumption input w. For $G(s) = (sI - A)^{-1}$ we recover $\mathcal{M}_0(G) = M_0(A)$.

Along with disturbances of finite consumption, $w \in L^1$, it also makes sense to consider finite energy perturbations $w \in L^2$, which may be thought of as representing noise, or time-domain bounded $w \in L^\infty$, which stand for persistent perturbations, as naturally all those could be the reason why trajectories of (1) or (3) get outside the region of attraction. Ability of a system to withstand destabilizing disturbances is referred to as *resilience*, and along with $\mathcal{M}_0(G)$ other ways to quantify it have been discussed, see e.g. [25]. Mitigating large transients is a general concern in control design, and has been addressed in various ways. LMI approaches are discussed in [12, 48], and a comparison between minimization of (4) and LMI techniques is [39], suggesting that, in the case study of plane Poiseuille flow, minimization (4) may be less conservative.

The remainder of this article is organized as follows. In Section 2, we introduce a frequency-domain approximation of $\mathcal{M}_0(G)$, better suited for the purpose of optimization, called the Kreiss system norm $\mathcal{K}(G)$. In a technical Section 3, estimates between various system norms related to L_1-disturbances are obtained, while Section 4 addresses the case of persistent perturbations. Experiments in Sections 5 and 6 focus on L_1-disturbances, where we apply Kreiss norm minimization to control nonlinear dynamics involving limit cycles, chaos or multiple fixed points, with the goal to increase the region of local stability or to even achieve global stability in closed loop. Conclusions are given in Section 7.

2. Kreiss system norm

A difficulty already mentioned in [28] is that $M_0(A)$, and similarly $\mathcal{M}_0(G)$, is hard to compute, let alone optimize. In response, the authors of [28] propose to use the *Kreiss constant* $K(A)$ of a matrix $A \in \mathbb{R}^{n\times n}$ as an alternative measure of normality. The latter is defined as

$$K(A) = \max_{\mathrm{Re}(s)>0} \mathrm{Re}(s)\overline{\sigma}\left((sI - A)^{-1}\right), \tag{5}$$

and its computation was investigated in [34, 35, 8]. By the famous Kreiss Matrix Theorem [45, p. 151, p.183] the estimate

$$K(A) \leq M_0(A) \leq enK(A)$$

is satisfied, where the constant is generally pessimistic, but sharp as shown in [28].

It turns out that minimizing $K(A)$ has an effect similar to minimizing $M_0(A)$, and this is in line with the observation that the global minimum $K(A) = M_0(A) = 1$ is the same for both criteria and occurs for normal A, and more generally, for matrices A where e^{At} is a contraction in the spectral norm. In [8] we have shown that optimizing $K(A_{\rm cl})$ is numerically possible, and that it has indeed the desired effect of driving $A_{\rm cl}$ closer to normal behavior.

Computing and optimizing $\mathcal{M}_0(G)$ in closed loop encounters the same difficulties as $M_0(A)$, and it is therefore tempting to consider the Kreiss system norm

$$\mathcal{K}(G) := \sup_{\mathrm{Re}(s)>0} \mathrm{Re}(s)\overline{\sigma}\left(C(sI - A)^{-1}B\right),$$

as it generalizes $K(A)$ in a natural way and satisfies the same estimate

$$\mathcal{K}(G) \leq \mathcal{M}_0(G) \leq en\,\mathcal{K}(G), \tag{6}$$

as we shall prove in Section 3.1. The principled reason to use $\mathcal{K}(G)$ is that its computation, and for that matter, optimization, may be based on a robust control technique, first proposed in [8, Thm. 2.1] for the case $B = C = I_n$:

Theorem 1. *Suppose A is stable. Then the Kreiss system norm $\mathcal{K}(G)$ can be computed through the robust H_∞-performance analysis program*

$$\mathcal{K}(G) = \max_{\delta\in[-1,1]} \left\| C\left(sI - \left(\tfrac{1-\delta}{1+\delta}A - I\right)\right)^{-1} B \right\|_\infty, \tag{7}$$

where $\|G\|_\infty$ denotes the H_∞-system norm. □

The Kreiss norm can be computed either by solving a non-smooth max-max program, or by a convex SDP; see [8, Theorems 2.1 and 2.4]. The SDP provides a certified accuracy, but the non-smooth technique is considerably faster. In numerical testing, we therefore use the SDP only for the final certification.

This leads us now to the following synthesis program:

$$\begin{array}{ll} \text{minimize} & \mathcal{K}(T_{wz}(\mathbf{x})) \\ \text{subject to} & K(\mathbf{x}) \text{ stabilizes } G \\ & \mathbf{x} \in \mathbb{R}^n \end{array} \tag{8}$$

where $\mathbf{x} \in \mathbb{R}^n$ are the finitely many tunable parameters of the structured controller $K(\mathbf{x})$, and where $T_{wz}(\mathbf{x}, s)$ is the closed-loop channel of (3) by which we assess transients. Program (8) may at leisure be complemented by adding standard H_∞- or H_2-loop-shaping requirements to further improve performances and robustness.

3. Norm estimates

In this Section, we obtain some basic estimates relating the Kreiss system norm $\mathcal{K}(G)$ to the $L^1 \to L^\infty$ induced norm $\mathcal{M}_0(G)$. We recall Young's inequality:

Lemma 1. (Young's inequality; see [13]). *Let $1/p + 1/q + 1/r = 2$, $p, q, r \geq 1$. Then*

$$\left| \iint f(x)g(x-y)h(y)dydx \right| \leq C_p C_q C_r \|f\|_p \|g\|_q \|h\|_r,$$

where

$$C_p = \left(p^{1/p}/p'^{1/p'}\right)^{1/2}, C_1 = C_\infty = 1.$$

□

Let ξ, η be test vectors of appropriate dimensions and consider a one-dimensional signal $u(t)$, then Lemma 1 gives

$$\begin{aligned} \xi^T C(sI - A)^{-1} B\eta\, u(s) &= \int_0^\infty e^{-st}(\xi^T C e^{At} B\eta * u)(t)dt \\ &\leq C_p C_q C_r \|e^{-ts}\|_p \|\xi^T C e^{At} B\eta\|_q \|u\|_r \\ &= C_p C_q C_r \mathrm{Re}(s)^{-1/p} p^{-1/p} \|\xi^T C e^{At} B\eta\|_q \|u\|_r, \end{aligned} \tag{9}$$

where $f(t) = e^{-st}$, $g(t) = \xi^T C e^{At} B\eta$, and $h(t) = u(t)$ are understood to take values 0 for $t < 0$. In the sequel we consider various choices of p, q, r.

3.1. **Kreiss system norm.** We apply Young's inequality with $r = 1$, $q = \infty$, $p = 1$, where $C_pC_qC_r = 1$. This leads to the following

Theorem 2. *For a stable system $G(s) = C(sI - A)^{-1}B$ we have the estimate*

$$\mathcal{K}(G) := \sup_{\mathrm{Re}(s)>0} \mathrm{Re}(s)\overline{\sigma}\left(C(sI-A)^{-1}B\right) \leq \sup_{t\geq 0} \overline{\sigma}\left(Ce^{At}B\right) =: \mathcal{M}_0(G). \tag{10}$$

Proof: From (9) with $r = 1$, $q = \infty$, $p = 1$, we get

$$\mathrm{Re}(s)|\xi^T C(sI-A)^{-1}B\eta\, u(s)| \leq \|\xi^T Ce^{At}B\eta\|_\infty \|u\|_1.$$

Now take $u_\epsilon(t) = \epsilon^{-1}$ on $[0, \epsilon]$, $u_\epsilon(t) = 0$ else. Then $\|u_\epsilon\|_1 = 1$. On the other hand, $u_\epsilon(s) \to 1$ as $\epsilon \to 0$, hence we get

$$\mathrm{Re}(s)|\xi^T C(sI-A)^{-1}B\eta| \leq \|\xi^T Ce^{At}B\eta\|_\infty = \sup_{t\geq 0} |\xi^T Ce^{At}B\eta|.$$

Now we consider test vectors $\xi \in \ell_2$, $\eta \in \ell_2$. Passing to the supremum over $\|\xi\|_2 \leq 1$, $\|\eta\|_2 \leq 1$ on the right gives

$$\begin{aligned}\mathrm{Re}(s)|\xi^T C(sI-A)^{-1}B\eta| &\leq \sup_{t\geq 0} \sup_{\|\xi\|_2,\|\eta\|_2\leq 1} |\xi^T Ce^{At}B\eta| \\ &= \sup_{t\geq 0} \overline{\sigma}\left(Ce^{At}B\right).\end{aligned}$$

Then taking the supremum over $\|\xi\|_2 \leq 1$, $\|\eta\|_2 \leq 1$ and $\mathrm{Re}(s) > 0$ on the left gives

$$\mathcal{K}(G) = \sup_{\mathrm{Re}(s)>0} \mathrm{Re}(s)\overline{\sigma}\left(C(sI-A)^{-1}B\right) \leq \sup_{t\geq 0} \overline{\sigma}\left(Ce^{At}B\right) = \mathcal{M}_0(G),$$

which is the claimed estimate. □

In order to interpret the expression $\mathcal{M}_0(G)$ on the right, we consider vector norms on $L^p([0,\infty), \mathbb{R}^n)$ defined as

$$\|u\|_{p,q} = \left(\int_0^\infty |u(t)|_q^p dt\right)^{1/p},$$

where $|u|_q = \left(\sum_{i=1}^n |u_i|^q\right)^{1/q}$ is the standard vector q-norm in $\mathbb{R}^n$, and where $\|u\|_{\infty,q} = \sup_{t\geq 0} |u(t)|_q$. Then, with the terminology introduced in [15],

$$\|G\|_{(q,s),(p,r)} = \sup_{u\neq 0} \frac{\|G * u\|_{q,s}}{\|u\|_{p,r}} \tag{11}$$

are induced norms $(L^p, \|\cdot\|_{p,r}) \to (L^q, \|\cdot\|_{q,s})$. In some cases these admit closed-form expressions, which is a prerequisite to making them amenable to computations, and even more so, optimization. By [15, (25)] one such case is

$$\|G\|_{(\infty,p),(1,r)} = \sup_{t\geq 0} \|G(t)\|_{p,r}, \tag{12}$$

where $\|A\|_{q,p} = \sup_{x\neq 0} \|Ax\|_q/\|x\|_p$ are the usual well-known induced matrix norms. Therefore, if we choose $p = r = 2$ in (12), then

$$\|G\|_{(\infty,2),(1,2)} = \sup_{t\geq 0} \|G(t)\|_{2,2} = \sup_{t\geq 0} \overline{\sigma}(G(t)) = \mathcal{M}_0(G).$$

We have proved

Proposition 1. *$\mathcal{M}_0(G)$ is an induced system norm. Given the vector input $w(t)$ satisfying $\int_0^\infty |w(t)|_2 dt = \int_0^\infty \left(\sum_{k=1}^p |w_k(t)|^2\right)^{1/2} dt = 1$, it measures the output $z = G*w$ by the vector signal norm*

$$\sup_{t\geq 0} \|z(t)\|_2 = \sup_{t\geq 0} \left(\sum_{i=1}^m |z_i(t)|^2\right)^{1/2}.$$

□

The norm $\mathcal{M}_0(G) = \|G\|_{(\infty,2),(1,2)}$ will be called the worst case transient peak norm, as it measures the peak of the time-domain response of G to a signal with finite resource consumption. Here 'response to a signal of finite resource consumption' is terminology adopted from [10].

In consequence, the expression $\mathcal{K}(G)$ is a frequency domain lower bound of $\mathcal{M}_0(G)$, and it is easy to see that $\mathcal{K}(G)$ is a norm, which we will call the *Kreiss system norm*.

Remark 1. We do not expect $\mathcal{K}(G)$ to be an induced system norm, but it does have the property of an operator norm, as follows from Theorem 1. Indeed, let $G_\delta = C(sI - (\frac{1-\delta}{1+\delta}A - I))^{-1}B$, then $\|G_\delta\|_\infty$ is the $L^2 \to L^2$ induced system norm when we take $\|\cdot\|_{2,2}$ as vector norm. Hence $\|z\|_{2,2} \leq \max_{\delta\in[0,1]} \|G_\delta\|_\infty \|w\|_{2,2}$, which due to (7) gives $\|G * w\|_{2,2} \leq K(G)\|w\|_{2,2}$.

Remark 2. Suppose $G = (A, B, C)$ is output controllable. Then for $y_0 \in \mathrm{im}(C)$, $y_0 \neq 0$, there exists u_0 and $t_0 > 0$ such that $Ce^{At_0}Bu_0 = y_0$. Then $\mathcal{M}_0(G) \geq \overline{\sigma}(Ce^{At_0}B) \geq \|Ce^{At_0}Bu_0\|_2/\|u_0\|_2 = \|y_0\|_2/\|u_0\|_2 > 0$. Some such condition is of course required, because if we take $C = [1\ 1]$, $B = \begin{bmatrix} 1 \\ -1 \end{bmatrix}$, $A = -I_2$, then $Ce^{At}B = 0$ for all t.

Remark 3. The famous estimate (upper bound due to Spijker [41])

$$K(A) \leq M_0(A) \leq neK(A) \tag{13}$$

holds for matrices A of size $n \times n$, and the global minimum $K(A) = M_0(A) = 1$ is attained for matrices where e^{At} is a contraction in the spectral norm, and in particular, for normal matrices. For this reason $M_0(A)$, and $K(A)$, have been considered as 'measures of non-normality' of a matrix.

The following extends (13), obtained in [26, 28, 41], to system norms:

Theorem 3. *We have*

$$\mathcal{K}(G) \leq \mathcal{M}_0(G) \leq en\mathcal{K}(G).$$

Proof: We have already shown in Theorem 2 that $\mathcal{K}(G) \leq \mathcal{M}_0(G)$. For the upper bound estimate, take test vectors ξ, η, then on putting $q(s) = \xi^T C(sI - A)^{-1}B\eta$, we have

$$\begin{aligned}
\xi^T Ce^{At}B\eta &= \frac{1}{2\pi j}\int_{\mathrm{Re}(s)=\mu} e^{st}\xi^T C(sI-A)^{-1}B\eta\, ds \text{ (inverse Laplace)} \\
&= -\frac{1}{2\pi j}\int_{\mathrm{Re}(s)=\mu} \frac{e^{st}}{t} q'(s) ds \text{ (partial integration)} \\
&= -\frac{1}{2\pi j}\frac{e^{\mu t}}{t}\int_{-\infty}^{\infty} e^{j\omega t} q'(\mu + j\omega) j\, d\omega \\
&= -\frac{e}{2\pi}\frac{1}{t}\int_{-\infty}^{\infty} |q'(1/t + j\omega)| d\omega = \frac{e}{2\pi}\mathrm{Re}(s)\|q'(\mathrm{Re}(s) + j\cdot)\|_1,
\end{aligned}$$

where in the last line we have chosen $\mathrm{Re}(s) = \mu = 1/t$. Since by [41] and [28] we have $\|q'\|_1 \leq 2\pi n \|q\|_\infty$, we find

$$\begin{aligned} |\xi^T C e^{At} B \eta| &\leq en\,\mathrm{Re}(s) \sup_\omega |\xi^T C((\mathrm{Re}(s) + j\omega)I - A)^{-1} B\eta| \\ &\leq en \sup_\omega \mathrm{Re}(s) |\xi^T C(sI - A)^{-1} B\eta|, \end{aligned}$$

so that taking the supremum over $\|\xi\|_2 = 1$, $\|\eta\|_2 = 1$ gives the right hand estimate. □

The question as to whether there exists a global bound attained by both criteria at the same 'normal' $G(s)$ is more involved. We have the following

Proposition 2. *We have the lower bound* $\overline{\sigma}(CB) \leq \mathcal{K}(G) \leq \mathcal{M}_0(G)$.

Proof: For $x > 0$ we have $\mathcal{K}(G) \geq x\overline{\sigma}(C(xI - A)^{-1}B) = \overline{\sigma}(Cx(xI - A)^{-1}B)$, and since the matrix $x(xI - A)^{-1}$ approaches I as $x \to \infty$, we get the lower bound $\overline{\sigma}(CB)$ all right. □

For $G = (sI - A)^{-1}$ this reproduces the bound $K(A) \geq 1$, which as we know is attained when e^{At} is a contraction in the spectral norm, and in particular, for normal matrices. The question is therefore whether, or for which systems $G = (A, B, C)$, the bound $\overline{\sigma}(CB)$ is attained. It is clear from Proposition 2 that $\mathcal{M}_0(G) = \overline{\sigma}(CB)$ implies equality $\overline{\sigma}(CB) = \mathcal{K}(G) = \mathcal{M}_0(G)$. However, in the matrix case the reverse argument is also true, i.e., $K(A) = 1$ implies $M_0(A) = 1$ as a consequence of the Hille-Yosida theorem [18]. The analogous result for systems is no longer valid.

Example 1. If we consider a stable SISO system

$$G(s) = \frac{c_{n-1}s^{n-1} + \cdots + c_0}{s^n + a_{n-1}s^{n-1} + \cdots + a_0}$$

then in controllable companion form

$$A = \begin{bmatrix} 0 & 1 & 0 & \dots & 0 \\ 0 & 0 & 1 & & \\ \dots & & & \ddots & \\ 0 & 0 & \dots & & 1 \\ -a_0 & -a_1 & & & -a_{n-1} \end{bmatrix}, B = \begin{bmatrix} 0 \\ \vdots \\ 0 \\ 1 \end{bmatrix}$$

$C = [c_0 \dots c_{n-1}]$. If the degree of the numerator is $n-1$, then we can normalize by taking the system G/c_{n-1}, then $\overline{\sigma}(CB) = 1$, and we may ask whether there are choices of the a_i, c_i where this bound is attained. However, if the degree of the numerator is $\leq n-2$, then always $CB = 0$, so here the lower bound is never attained.

This leaves now two situations. In case $\overline{\sigma}(CB) = 0$ one may wonder under what conditions $\mathcal{K}(G) = \mathcal{M}_0(G) > 0$ is satisfied, and whether this holds under normality of A. On the other hand, when $\overline{\sigma}(CB) > 0$ one may ask under what conditions the lower bound is attained, whether attainment $\overline{\sigma}(CB) = \mathcal{K}(G)$ implies attainment $\overline{\sigma}(CB) = \mathcal{M}_0(G)$, and again, whether this is linked to normality of A.

The following example shows that in the case $\overline{\sigma}(CB) = 0$, normality of A is no longer the correct answer.

Example 2. Take $C = [1\ 1]$, $B = \begin{bmatrix} 1 \\ -1 \end{bmatrix}$, $A = \begin{bmatrix} -\lambda & 0 \\ 0 & -\mu \end{bmatrix}$ with $0 < \lambda < \mu$. Then $\overline{\sigma}(CB) = 0$, but $Ce^{At}B = e^{-\lambda t} - e^{-\mu t} \neq 0$ for $t > 0$, so that $\mathcal{M}_0(G) > 0$, and by the Kreiss matrix theorem we also have $\mathcal{K}(G) > 0$. This also means that neither $\mathcal{M}_0$ not $\mathcal{K}$ are monotone in t. For $\lambda = 1$, $\mu = 2$ we obtain $\mathcal{K}(G) = 0.1716 < \mathcal{M}_0(G) = 0.25$,

In case $\overline{\sigma}(CB) > 0$, the situation is also fairly unsettled, as the following examples underline.

Example 3. Take $B = [0\ 0\ 1]^T$, $C = [1\ 1\ 1]$, $a_0 = 0.9608$, $a_1 = 1$, $a_2 = 1$, in the controllable companion form above, which gives $G = (s^2+s+1)/(s^3+s^2+s+0.9608)$, then $|CB| = 1$, $\mathcal{K}(G) = \mathcal{M}_0(G) = 1$. Here the lower bound is attained, while $K((sI-A)^{-1}) = 1.17$, $M_0((sI-A)^{-1}) = 1.43$, thus with A not a contraction, and in particular, not normal.

Example 4. We give an example of a normal matrix A, where $\overline{\sigma}(CB) > 0$, but $\mathcal{K} < \mathcal{M}_0$. Change Example 2 by putting $C = [1, 1]$, $B = [1; -1 + \epsilon]$. Then $\overline{\sigma}(CB) = \epsilon$. We get $Ce^{At}B = e^{-\lambda t} - (1-\epsilon)e^{-\mu t}$. With $\mu = 2$, $\lambda = 1$, $\epsilon = 0.25$ we get $0.25 = \overline{\sigma}(CB) < \mathcal{K}(G) = 0.3006 < \mathcal{M}_0(G) = 0.3333$.

Example 5. Now we give an example where $\mathcal{K}(G) = \overline{\sigma}(CB) = 1$, but $\mathcal{K}(G) < \mathcal{M}_0(G)$. Take $A = [-q, p; 0, -q]$, $B = [b_1; b_2]$, $C = [c_1, c_2]$ with $b_1c_1 + b_2c_2 = 1$. Then with the choices $q = 0.6509$, $p = 0.8746$, $C = [-19.5450, -19.1251]$, $B = [-0.2592; 0.2126]$, we get $\mathcal{K}(G) = 1 < \mathcal{M}_0(G) = 1.72$.

Example 6. The failure in Example 5 is again not related to failure of normality of A, because the same may occur with diagonal A as seen with $G(s) = \dfrac{s - 2.032}{s^2 + 0.8456s + 0.1769}$.

Example 7. Example 5 can be used to analyze the special case considered in [8], where the C-matrix is $J = [I_n, 0]$ and the B-matrix is J^T. Starting out from the system in Example 5, we have to find a regular 2×2 matrix T such that $CT^{-1} = [1, 0] = J$ and $TB = [1; 0] = J^T$. That requires $t_{11} = c_1$, $t_{12} = c_2$ and $c_1b_1 + c_2b_2 = 1$. Moreover, we need to fix t_{21}, t_{22} such that $t_{21}b_1 + t_{22}b_2 = 0$. That gives for $b_1 \neq 0$:

$$T = \begin{bmatrix} c_1 & c_2 \\ -\frac{t_{22}b_2}{b_1} & t_{22} \end{bmatrix}$$

which is regular for $t_{22} \neq 0$. Now $G = Ce^{At}B = CT^{-1}Te^{At}T^{-1}TB = Je^{TAT^{-1}t}J^T$, where A is as in the previous example. Then we have $1 = \mathcal{K}(G) < \mathcal{M}_0(G)$, so the special structure $C = B^T = J$ used in [8] does not help.

Example 8. The case $C = I$ does not help either. Let $A = [-0.0939, 1.0000; 0, -0.0939]$, $B = [0.4722, 0.7973; 0.0339, 0.5553]$, $C = I_2$, then $\overline{\sigma}(CB) = 1.0577 < \mathcal{K}(G) = 1.9634 < \mathcal{M}_0(G) = 2.5226$.

Example 9. As we have seen even for SISO systems with normal matrix A, we cannot expect to get equality $\mathcal{K}(G) = \mathcal{M}_0(G) = \overline{\sigma}(CB)$. There is, however, a special case when A is diagonalizable with real eigenvalues and all c_ib_i have equal signs, say $c_ib_i > 0$. Then by Laguerre's theorem the exponential polynomial $\sum_{i=1}^n -\lambda_i c_i b_i e^{-\lambda_i t}$ does not change sign, hence the curve $M(t) = \sum_{i=1}^n c_i b_i e^{\lambda_i t}$ has no extrema and is therefore monotone decreasing, in which case the maximum is attained at $t = 0$ with value $\sum_{i=1}^n c_i b_i$.

Remark 4. In the same vein, we also mention conditions given in [44], under which any induced system norm attains the value $\overline{\sigma}(CB)$. Since this applies to $\mathcal{M}_0(G)$, this line gives cases of attainment.

Remark 5. Hausdorff's numerical abscissa $\omega(A)$ satisfies $\|e^{tA}\| \leq e^{\omega(A)t}$, hence e^{tA} is a contraction semigroup iff $\omega(A) \leq 0$. Since $\omega(A) = \frac{d}{dt}\|e^{tA}\|\Big|_{t=0}$, the slope of the curve $t \mapsto \|e^{tA}\|$ at $t = 0$ in that case conveys global information on the entire curve, and the semigroup e^{tA}. This is why in the fluid flow literature it has been suggested that minimizing $\omega(A(K))$ in closed loop might be a way to prevent transition to turbulence [47, 46, 45, 22, 40, 32]. Due to $\omega(A) = \frac{1}{2}\overline{\lambda}(A + A^T)$ this would have the additional advantage

of being an eigenvalue optimization problem, easier to handle than (8). However, in [8] we demonstrated that minimizing $\omega(A(K))$ in closed loop does not have the desired effect of reducing transients.

One way to extend $\omega(A)$ to systems is $\omega(G) = \frac{d}{dt}\|Ce^{tA}B\|\Big|_{t=0}$, because then $\omega(G) \leq 0$ continues to be a necessary condition for attainment $\mathcal{M}_0(G) = \overline{\sigma}(CB)$. However, unlike the matrix case, it is no longer sufficient. Before showing this, we address necessity of attainment for the Kreiss norm:

Proposition 3. *A necessary condition for attainment of the lower bound $\mathcal{K}(G) = \overline{\sigma}(CB)$ is $\overline{\lambda}(Y + Y^T) \leq 0$, where $Y = Q^TCABB^TC^T$, and where the columns of Q form an orthonormal basis of the maximum eigenspace of CBB^TC^T.*

Proof: Let $A(\eta) = \frac{\eta}{2-\eta}A - I$ and put $G(\eta, s) = C(sI - A(\eta))^{-1}B$, then (7) can be rewritten as $\mathcal{K}(G) = \max_{\eta\in[0,2]} \|G(\eta,\cdot)\|_\infty$. Now $\eta = 0$ contributes the value $\overline{\sigma}(CB)$ to the maximum over $\eta \in [0, 2]$, because $A(0) = -I$, and therefore $G(0, s) = C(sI - A(0))^{-1}B = (s + 1)^{-1}CB$, hence $\|G(0,\cdot)\|_\infty = \max_\omega |(j\omega + 1)^{-1}|\,\overline{\sigma}(CB) = \overline{\sigma}(CB)$, attained at the single frequency $\omega = 0$. In consequence, due to our hypothesis $\mathcal{K}(G) = \overline{\sigma}(CB) > 0$, the slope of $\phi : \eta \mapsto \|G(\eta,\cdot)\|_\infty$ at $\eta = 0$ must be non-positive, as otherwise $\|G(\eta,\cdot)\|_\infty = \|C(sI - A(\eta))^{-1}B\|_\infty$ would attain values $> \overline{\sigma}(CB)$ for some small $\eta > 0$.

To compute $\phi'(0)$, observe that since $\|G(0,\cdot)\|_\infty$ is attained at the single frequency $\omega = 0$, we have

$$\begin{aligned}
\phi'(0) &= \|\cdot\|_\infty{}'(G(h,\cdot), \tfrac{d}{d\eta}G(\eta,\cdot))\Big|_{\eta=0} = \overline{\sigma}'(G(\eta, j0), \tfrac{d}{d\eta}G(\eta, j0))\Big|_{\eta=0} \\
&= \overline{\sigma}'(CB, -C(A(\eta)^{-1}\tfrac{d}{d\eta}A(\eta)A(\eta)^{-1})B)\Big|_{\eta=0} = \overline{\sigma}'(CB, C\tfrac{1}{2}AB) \\
&= \tfrac{1}{4}\,\overline{\lambda}(Q^H(CAB)P + P^H(B^TA^TC^T)Q) \\
&= \frac{1}{4\overline{\sigma}(CB)}\overline{\lambda}(Q^TC(ABB^T + BB^TA^T)C^TQ),
\end{aligned}$$

where the second line uses $\frac{d}{d\eta}\,[A(\eta)^{-1}] = -A(\eta)^{-1}\frac{d}{d\eta}A(\eta)A(\eta)^{-1} = -A(\eta)^{-1}\frac{2}{(2-\eta)^2}AA(\eta)^{-1}$, which at $\eta = 0$ gives $-\frac{1}{2}A$, whereas the third line uses Corollary 3 based on a SVD $G(0,0) = CB = \begin{bmatrix}Q & R\end{bmatrix}\begin{bmatrix}\overline{\sigma}(CB)I & \\ & \Sigma\end{bmatrix}\begin{bmatrix}P^T \\ T^T\end{bmatrix}$. The last line follows by re-substituting $Q^HCB = \overline{\sigma}(CB)P^H$. □

Note that this leads back to $\omega(A) \leq 0$ for $C = B = I$.

Lemma 2. *The Clarke subdifferential of the maximum singular value function is $\partial\overline{\sigma}(G) = \{QYP^H : Y \succeq 0, \mathrm{Tr}(Y) = 1\}$, where $G = \begin{bmatrix}Q & R\end{bmatrix}\begin{bmatrix}\overline{\sigma}(G) & \\ & \Sigma\end{bmatrix}\begin{bmatrix}P^H \\ T^H\end{bmatrix}$ is a SVD of G.*

Proof: From $\overline{\sigma}(G)^2 = \overline{\lambda}(GG^H)$ we get $2\overline{\sigma}(G)\partial\overline{\sigma}(G) = F'(G)^*\partial\overline{\lambda}(F(G))$, where $F : \mathbb{M}^{n,m} \to \mathbb{S}^m$ is the mapping $F(X) = XX^H$. Now $\partial\overline{\lambda}(GG^H) = \{QYQ^H : Y \succeq 0, \mathrm{Tr}(Y) = 1\}$, where the columns of Q in the SVD form an orthonormal basis of the maximum eigenspace of GG^H. Furthermore, $F'(G)D = GD^H + DG^H$, hence for a test vector $S \in \mathbb{S}^m$ we have by the definition of the adjoint $\langle D, F'(G)^*S\rangle = \langle F'(G)D, S\rangle = \mathrm{Re}\,\mathrm{Tr}\,S(GD^H + DG^H) = 2\mathrm{Re}\,\mathrm{Tr}\,SDG^H = 2\mathrm{Re}\,\mathrm{Tr}\,(SG)^HD = \langle D, 2SG\rangle$, so that the action of the adjoint is $F'(G)^*S = 2SG$. On substituting $S = QYQ^H \in \partial\overline{\lambda}(GG^H)$, we obtain $\partial\overline{\sigma}(G) = \frac{1}{2\overline{\sigma}(G)}\{2QYQ^HG : Y \succeq 0, \mathrm{Tr}(Y) = 1\}$. Now since $Q^HG = \overline{\sigma}(G)P^H$ from the SVD, we obtain the claimed $\partial\overline{\sigma}(G) = \{QYP^H : Y \succeq 0, \mathrm{Tr}(Y) = 1\}$. □

Lemma 3. *The Clarke directional derivative is* $\overline{\sigma}'(G,D) = \frac{1}{2}\overline{\lambda}(Q^H DP + P^H D^H Q)$.

Proof: We have $\overline{\sigma}'(G,D) = \max\{\langle \Phi, D\rangle : \Phi \in \partial\overline{\sigma}(G)\} = \max\{\mathrm{Re}\,\mathrm{Tr}\,\Phi^H D : \Phi \in \partial\overline{\sigma}(G)\} = \max\{\mathrm{Re}\,\mathrm{Tr}\,PYQ^H D : Y \succeq 0, \mathrm{tr}(Y) = 1\} = \max\{\frac{1}{2}\mathrm{Re}\,\mathrm{Tr}\,Y(Q^H DP + P^H D^H Q) : Y \succeq 0, \mathrm{Tr}(Y) = 1\} = \frac{1}{2}\overline{\lambda}(Q^H DP + P^H D^H Q)$. □

On re-substituting $Q^H G = \overline{\sigma}(G)P^H$, we can also write this in the form $\overline{\sigma}'(G,D) = \frac{1}{2\overline{\sigma}(G)}\overline{\lambda}(Q^H DG^H Q + Q^H GD^H Q) = \frac{1}{2\overline{\sigma}(G)}\overline{\lambda}(Q^H \left[DG^H + GD^H\right] Q)$.

The following is an immediate consequence of the finite maximum rule for the subdifferential.

Lemma 4. *Suppose* $\|G\|_\infty$ *is attained at the finitely many frequencies* $\omega_1, \ldots, \omega_r$. *Then* $\partial\|\cdot\|_\infty(G) = \{\sum_{k=1}^r Q_k Y_k P_k^H : Y_k \succeq 0, \sum_{k=1}^r \mathrm{Tr}(Y_k) = 1\}$, *where for every* k *we let* $G(j\omega_k) = \begin{bmatrix} Q_k & R_k \end{bmatrix} \mathrm{diag}(\|G\|_\infty, \Sigma_k) \begin{bmatrix} P_k & T_k \end{bmatrix}^H$ *be a SVD of* $G(j\omega_k)$. □

One also immediately gets the following description of the Clarke directional derivative of the H_∞-norm:

Lemma 5. *Suppose* $\|G\|_\infty$ *is attained at the finitely many frequencies* $\omega_1, \ldots, \omega_r$. *Then* $\|\cdot\|'_\infty(G,D) = \max_{k=1,\ldots,r} \frac{1}{2}\overline{\lambda}(Q_k^H DP_k + P_k^H D^H Q_k)$, *with* P_k, Q_k *the same as above.* □

Remark 6. Formulas for subgradients and directional derivatives of the H_∞-norm have first been given in [3, 4, 5, 6]. Using the SVD as in Lemma 2 is numerically preferable to formulas using the subdifferential $\partial\overline{\lambda}$ directly, and we exploited this favorably in the implementation of `hinfstruct` and `systune` [33].

Corollary 1. *Condition* $\overline{\lambda}(Y + Y^T) \leq 0$ *is also necessary for attainment of the lower bound* $\mathcal{M}_0(G) = \overline{\sigma}(CB)$. *Moreover, when* $C = B = I$, *this condition is also sufficient.*

Proof: The first part of the statement follows from (3) in tandem with Proposition 3. One may also obtain it directly by computing $\frac{d}{dt}\|Ce^{tA}B\|\Big|_{t=0} = \overline{\sigma}'(CB, CAB) = \frac{1}{2\overline{\sigma}(CB)}\overline{\lambda}(Q^T(CABB^TC^T + CBB^TATC^T)Q) = \frac{1}{2\overline{\sigma}(CB)}\overline{\lambda}(Y + Y^T)$ using Lemma 3.

For $C = B = I$ we have $Q = I$, hence $\overline{\lambda}(Y + Y^T) = \overline{\lambda}(A + A^T) = 2\omega(A)$, but $\omega(A) \leq 0$ is the classical necessary *and* sufficient condition for a contraction semi-group. □

Example 10. Now we show that the necessary condition $\overline{\lambda}(Y + Y^T) \leq 0$ is in general not sufficient, which contrasts with the case $C = B = I$, where this is true. We take $A = \begin{bmatrix} 0 & 1 \\ -6 & -5 \end{bmatrix}$, $B = \begin{bmatrix} 0 \\ 1 \end{bmatrix}$, $C = \begin{bmatrix} -10 & 1 \end{bmatrix}$, where one gets $1 = \overline{\sigma}(CB) = \mathcal{K}(G) < \mathcal{M}_0(G) = 1.5148$, $\omega(G) = -30$ with $\overline{\lambda}(Y + Y^T) = -30$, confirming that the condition is necessary for attainment of the Kreiss norm, but not sufficient for attainment of the transient amplification.

Another case is $A = \begin{bmatrix} 0 & 1 \\ -5 & -1 \end{bmatrix}$, $B = \begin{bmatrix} 0 \\ 1 \end{bmatrix}$, $C = \begin{bmatrix} -8 & 1 \end{bmatrix}$, which gives $\overline{\sigma}(CB) = 1 < \mathcal{K}(G) = 1.13$ with $\overline{\lambda}(Y + Y^T) = -18$, showing that the condition is neither sufficient for attainment of the Kreiss norm, nor of transient amplification.

We do not know whether there are cases with $\overline{\sigma}(CB) < \mathcal{K}(G) = \mathcal{M}_0(G)$.

3.2. **More vector norms.** The discussion in Section 3.1 considers $\mathcal{M}_0(G)$ as induced norm $G : (L^1, \|\cdot\|_{1,2}) \to (L^\infty, \|\cdot\|_{\infty,2})$, with the appropriate choice of the ℓ_2-norm as

vector norm. However, (12) shows that various other choices of vector norms could lead to numerically exploitable expressions $\mathcal{K}, \mathcal{M}$. Choosing test vectors $\xi \in \ell_{p'}$, $\eta \in \ell_r$ gives

$$\sup_{\mathrm{Re}(s)>0} \mathrm{Re}(s)\|C(sI-A)^{-1}B\|_{r,p} \leq \sup_{t\geq 0} \|Ce^{At}B\|_{r,p},$$

where $\|M\|_{r,p}$ is the $\ell_p \to \ell_r$ induced matrix norm. This may lead to other criteria compatible with the goal to sensing $L^1 \to L^\infty$ amplification. Tractable expressions are obtained e.g. for $p=1$, $r=\infty$, which corresponds to taking $\xi \in \ell_1$, $\eta \in \ell_1$. Here we get the estimate

$$\sup_{\mathrm{Re}(s)>0} \max_{ik} \left|c_i \mathrm{Re}(s)(sI-A)^{-1}b_k\right| \leq \sup_{t\geq 0} \max_{ik} \left|c_i e^{At} b_k\right|$$

which reads as

$$\max_{ik} \mathcal{K}(c_i e^{A\bullet} b_k) \leq \max_{ik} \mathcal{M}_0(c_i e^{A\bullet} b_k)$$

with a finite maximum of SISO Kreiss constants and transient growth norms involved. This practical entry-wise Kreiss norm offers potential to weigh some channels more than others. An upper bound of $\mathcal{M}_0$ is readily obtained as $en \max_{ik} \mathcal{K}(c_i e^{A\bullet} b_k)$ from Theorem 3.

3.3. **Other vector norms: ℓ_∞.** Now take (9), but with $|\xi|_\infty \leq 1, |\eta|_\infty \leq 1$. We get on the right

$$|\xi^T(Ce^{At}B)\eta| \leq \|(Ce^{At}B)\eta\|_1 \leq \|Ce^{At}B\|_{1,\infty}$$

because the dual norm to ℓ_∞ is ℓ_1. However, this norm is not very helpful for matrices with large dimension m, because for $A \in \mathbb{R}^{m\times n}$, we have:

$$\|A\|_{1,\infty} = \max_{r\in\{-1,1\}^m} \|Ar\|_1.$$

With the above technique, we easily get the following estimate

$$\max_{r\in\{-1,1\}^m} \mathcal{K}(Gr) \leq \max_{r\in\{-1,1\}^m} \mathcal{M}_0(Gr).$$

4. Peak-to-peak norm for persistent perturbations

In this section, we discuss the choice $p=\infty$, $q=r=1$ in Young's inequality (9), which will allow us to address the case of persistent perturbations w in (3), when for an input $\|w\|_{\infty,\infty} \leq 1$, we measure the response by the same signal norm $\|G*w\|_{\infty,\infty}$. For test vectors ξ, η and a one-dimensional signal u we get from (9)

$$|\xi^T C(sI-A)^{-1}B\eta\, u(s)| \leq \|e^{-st}\|_\infty \|\xi^T Ce^{At}B\eta\|_1 \|u\|_1 = \|\xi^T Ce^{At}B\eta\|_1 \|u\|_1.$$

Letting the scalar signal $u(t)$ of unit L_1-norm approach the δ-distribution, we get

$$|\xi^T C(sI-A)^{-1}B\eta| \leq \|\xi^T Ce^{At}B\eta\|_1 = \int_0^\infty |\xi^T Ce^{At}B\eta| dt.$$

Now let m be the number of outputs, p the number of inputs, and let $g_{ik}(t)$ be the entries of the matrix $Ce^{At}B$, then with $\|\xi\|_2 \leq 1$ and $\|\eta\|_2 \leq 1$ we get

$$\begin{aligned}
\int_0^\infty |\xi^T Ce^{At}B\eta|dt &= \int_0^\infty \left|\sum_{i=1}^m \sum_{k=1}^p \xi_i g_{ik}(t)\eta_k\right| dt \\
&\leq \sum_{i=1}^m |\xi_i| \sum_{k=1}^p |\eta_k| \int_0^\infty |g_{ik}(t)|dt \\
&= \sum_{i=1}^m |\xi_i| \sum_{k=1}^p \|g_{ik}\|_1 |\eta_k| \\
&\leq \left(\sum_{i=1}^m |\xi_i|^2\right)^{1/2} \left(\sum_{i=1}^m \left(\sum_{k=1}^p \|g_{ik}\|_1|\eta_k|\right)^2\right)^{1/2} \\
&\leq \left(m \max_{i=1,\ldots,m} \left(\sum_{k=1}^p \|g_{ik}\|_1\right)^2\right)^{1/2} = \sqrt{m} \max_{i=1,\ldots,m} \sum_{k=1}^p \|g_{ik}\|_1.
\end{aligned}$$

When we recall that the time-domain peak-to-peak, or peak-gain, system norm is defined as

$$\|G\|_{\mathrm{pk\_gn}} = \max_{u\neq 0} \frac{\|G*u\|_{\infty,\infty}}{\|u\|_{\infty,\infty}} = \max_{i=1,\ldots,m} \sum_{j=1}^p \|g_{ij}(t)\|_1,$$

then we have shown the estimate $\|G\|_\infty \leq \sqrt{m}\|G\|_{\mathrm{pk\_gn}}$ for a system G with m outputs. Since in this case input signals do not have to vanish at infinity, this estimate holds also when G has direct transmission. More generally even, as no structure of the g_{ij} is used, the estimate remains true when $g_{ik} \in L^1([0,\infty), \mathbb{R}^n)$, and this can be extended to $(m \times p)$-valued Radon measures.

Let us now look at the reverse estimate, which is analogous to the right hand estimate in the Kreiss matrix theorem (Theorem 3). Consider a stable finite-dimensional strictly proper system

$$G: \quad \begin{aligned} \dot{x} &= Ax + Bu \\ y &= Cx \end{aligned}$$

where $G(t) = Ce^{At}B$. Let $g_{ij}(t) = c_i e^{At} b_j$, where c_i is the ith row of C, b_j the jth column of B, then $\|G\|_{\mathrm{pk\_gn}} = \max_{i=1,\ldots,m} \sum_{j=1}^p \|g_{ij}\|_1 = \sum_{j=1}^p \|c_i e^{At} b_j\|_1$ for some i.

We now relate the peak-gain norm to the Hankel singular values of G. The following was proved in the SISO case $p = m = 1$ in [11, Thm. 2] for discrete systems, and in [17, pp. 11-12] for continuous SISO systems, where in the latter reference the idea of proof is attributed to I. Gohberg.

Lemma 6. *Let G be real-rational, strictly proper and stable, with p outputs and McMillan degree n. Then*

$$\|G\|_{\mathrm{pk\_gn}} \leq 2p^{1/2} \left(\sigma_{H1} + \cdots + \sigma_{Hn}\right), \tag{14}$$

where σ_{Hi} are the Hankel singular values of G. In particular, $\|G\|_{\mathrm{pk\_gn}} \leq 2np^{1/2}\|G\|_\infty$.

Proof: We have for the $i \in \{1, \ldots, m\}$ where the maximum is attained

$$\begin{aligned}
\|G\|_{\text{pk_gn}} &= \sum_{j=1}^{p} \|c_i e^{At} b_j\|_1 = 2\sum_{j=1}^{p} \int_0^\infty \left|c_i e^{2A\tau} b_j\right| d\tau = 2\int_0^\infty \sum_{j=1}^{p} \left|\text{Tr}(e^{A^T t} c_i^T)^T (e^{At} b_j)\right| dt \\
&= 2\int_0^\infty \sum_{j=1}^{p} \left|\sum_{\ell=1}^{n^2} \text{vec}(e^{A^T t} c_i^T)_\ell \cdot \text{vec}(e^{At} b_j)_\ell\right| dt \\
&\leq 2\left(\int_0^\infty \sum_{j=1}^{p}\sum_{\ell=1}^{n^2} |\text{vec}(e^{A^T t} c_i^T)_\ell|^2 dt\right)^{1/2} \left(\int_0^\infty \sum_{j=1}^{p}\sum_{\ell=1}^{n^2} |\text{vec}(e^{At} b_j)_\ell|^2 dt\right)^{1/2} \\
&= 2\left(\int_0^\infty \sum_{j=1}^{p} \text{Tr}(e^{A^T t} c_i^T c_i e^{At}) dt\right)^{1/2} \left(\int_0^\infty \sum_{j=1}^{p} \text{Tr}(e^{At} b_j b_j^T e^{A^T t}) dt\right)^{1/2} \\
&= 2p^{1/2}\left(\int_0^\infty \text{Tr}(e^{A^T t} c_i^T c_i e^{At}) dt\right)^{1/2} \left(\int_0^\infty \text{Tr}(e^{At} B B^T e^{A^T t}) dt\right)^{1/2}.
\end{aligned}$$

Recall that the observability and controllability Gramians of the system G are

$$W_o = \int_0^\infty e^{A^T t} C^T C e^{At} dt, \quad W_c = \int_0^\infty e^{At} B B^T e^{A^T t} dt.$$

Now $\text{Tr}\int_0^\infty e^{A^T t} c_i^T c_i e^{At} dt \leq \text{Tr}\int_0^\infty e^{A^T t} C^T C e^{At} dt$ follows from $c_i^T c_i \preceq C^T C$ by applying a congruence transformation with e^{At}. Hence $\|G\|_{\text{pk\_gn}} \leq 2p^{1/2}\left[\text{Tr}(W_o)\text{Tr}(W_c)\right]^{1/2}$. Now if we take a balanced realization, then $W_o = W_c = \text{diag}(\sigma_{H1}, \ldots, \sigma_{Hn})$ for the Hankel singular values $\sigma_{H_1} \geq \cdots \geq \sigma_{Hn}$, hence $\|G\|_{\text{pk\_gn}} \leq 2\sqrt{p}(\sigma_{H1} + \cdots + \sigma_{Hn}) \leq 2p^{1/2} n\sigma_{H1} \leq 2p^{1/2} n\|G\|_\infty$ for a system without direct transmission. This uses $\sigma_{H1} \leq \|G\|_\infty$. □

Note, however, that by the Enns-Glover bound we have

$$\|G\|_\infty \geq \max\{\overline{\sigma}(D), \sigma_{H1}\}$$

for the maximum Hankel singular value σ_{H1} of $G = (A, B, C, D)$, so this holds also for systems with direct transmission. Indeed, if we define the Hankel semi-norm of a system G as

$$\|G\|_H = \sup\left\{\frac{\|G * u\|_{L^2(T,\infty)}}{\|u\|_{L^2[0,T]}} : T > 0, u \in L^2[0,\infty)\right\},$$

then $\|G\|_H = \sigma_{H1}$ for the maximum Hankel singular value. But with this formulation, it is immediate to see that $\|G\|_H \leq \|G\|_\infty$, when we recall that $\|G\|_\infty$ is the L^2-operator norm.

Therefore we get for a system with direct transmission

$$\|G\|_{\text{pk\_gn}} \leq \|G - D\|_{\text{pk\_gn}} + \|\!|D|\!\|_\infty \leq 2p^{1/2} n\sigma_{H1} + p^{1/2}\overline{\sigma}(D) \leq (2n+1)p^{1/2}\|G\|_\infty$$

using the fact that $\sigma_{H1} \leq \|G\|_\infty$ and $\overline{\sigma}(D) \leq \|G\|_\infty$. Altogether, we have proved the following estimates for the H_∞- and peak-gain norms stated in [9]:

Theorem 4. *Let G be a stable real-rational system with n poles, p inputs and m outputs. Then*

$$m^{-1/2}\|G\|_\infty \leq \|G\|_{\text{pk\_gn}} \leq (2n+1)p^{1/2}\|G\|_\infty.$$

A large variety of synthesis experiments based on the peak-gain norm $\|G\|_{\text{pk\_gn}}$ has been presented in [9], so that our experiments here may focus on L_1-disturbances.

4.1. **Noise as perturbation.** In this section we consider the case $w \in L^2$, $G * w \in L^\infty$, where we can rely on [15]. Consider for instance $\|G\|_{(\infty,2)(2,2)} = \lambda_{\max}(CQC^T)$, where $Q \succeq 0$ is the unique solution of the Lyapunov equation $AQ + QA^T + BB^T = 0$. This norm can be optimized directly using a technique similar to [16].

5. Applications to nonlinear dynamics with limit cycle attractor

In this section and the following, we consider applications illustrating the use of the Kreiss system norm for both analysis and feedback control design. The techniques are general and applicable to a large variety of nonlinear controlled systems. We recall that in all tests the results are certified aposteriori, as Kreiss norm optimization is based on a heuristic.

5.1. **Study of 2nd-order dynamics with limit cycle attractor.** We start with the model of Brunton and Noack [14], which is a low-order illustration of a dynamic mechanisms known in oscillator flow, observed for instance on a larger scale in Navier-Stokes equations. Examples of this type include fluid flow around a cavity or a cylinder [27, 23]. The model is of the form

$$\left\{ \begin{array}{rcl} \dot{x} & = & \begin{bmatrix} \sigma_u & -\omega_u \\ \omega_u & \sigma_u \end{bmatrix} x + B_w w + Bu \\ w & = & \phi(x) \\ y & = & Cx \end{array} \right. , \tag{15}$$

with $B_w := I$, $B := [0\ g]^T$ $C := [0\ 1]$,

$$\phi(x) := \alpha_u \|x\|^2 \begin{bmatrix} -\beta_u & -\gamma^u \\ \gamma_u & -\beta_u \end{bmatrix} x \,,$$

and $\alpha_u, \beta_u > 0$. Signals u and y are control input and measured output, respectively. It is easy to verify that the triple (A, B, C) is stabilizable and detectable.

Unlike transitional amplifier flows, oscillator flows are characterized by an unstable fixed point at the origin and a globally attractive limit cycle, here with radius $\sqrt{\sigma_u/\alpha_u\beta_u}$. This is shown in Fig. 1 for two initial conditions inside and outside the asymptotic limit cycle for data $\alpha_u = 1$, $\beta_u = 1$, $\omega_u = 1$, $\gamma_u = 0$, $\sigma_u = 0.1$ and $g = 1$.

The goal is to compute a feedback controller $u = K(s)y$ with two main design requirements. Firstly, K has to stabilize the origin, often called the base flow. Secondly, trajectories trapped in the limit cycle should be driven back to the origin with limited oscillations. Additional insight into this model in terms of fluid flow interpretation can be found in [14].

In order to mitigate the effects of nonlinearity, we minimize the Kreiss system norm in closed loop. This leads to the following min-max constrained program

$$\begin{array}{ll} \text{minimize} & \max\limits_{\delta\in[-1,1]} \left\| J^T \left(sI - \left(\frac{1-\delta}{1+\delta} A_{cl}(K) - I\right)\right)^{-1} J \right\|_\infty \\ \text{subject to} & K \text{ robustly stabilizing, } K \in \mathscr{K} \\ & \alpha(A_{cl}(K)) \le -\eta \\ & \|W(s)GK(I+GK)^{-1}\|_\infty \le 1\,. \end{array} \tag{16}$$

Here $K \in \mathscr{K}$ means that the controller has a prescribed structure, which could be a PID, observed-based or low-order controller, a decentralized controller, as well as any control architecture assembling simple control components. The robust stability constraint on K in (16) demands stability of the entire set of matrices $\left\{ \frac{1-\delta}{1+\delta} A_{cl} - I : \ \delta \in [-1,1] \right\}$, and in particular, for $\delta = 0$ that of $A_{cl}(K)$. Matrix J is a restriction matrix to the space of physical plant states since transient amplification of controller states is not relevant.

We have $J := I_n$ for a static feedback controller and $J := [I_n,\, 0_{n\times n_K}]^T$ for an n_K-order output-feedback controller (see also Examples 7,8).

The notation $\alpha(\cdot)$ refers to the spectral abscissa, and the constraint $\alpha(A_{cl}) \le -\eta$ in (16) therefore imposes a convergence rate to the origin for the linear dynamics in closed loop. In our experiments we have chosen $\eta = 0.1$.

Remark 7. Program (16) is a special case of a much wider class of problems with parametric uncertainty discussed in [2, 7], where a successful approach alternating between two non-smooth programs is used. The inner max-max program with controller K fixed is characterized by a light form of non-smoothness and can be addressed by a first-order non-smooth trust-region technique whose convergence certificates have been established in [7]. The outer min-max program with δ fixed corresponds to a more severe form of non-smoothness and should be handled by dedicated bundle or bundle trust-region techniques [7, 5, 6].

These constraints are readily implemented from the closed-loop nonlinear system:

$$\dot{x}_{cl} \;=\; A_{cl}x_{cl} + B_{w,cl}\phi_{cl}(x_{cl}), \quad x_{cl} := [x^T, x_K^T]^T\,, \tag{17}$$

where

$$A_{cl} := \begin{bmatrix} A + BD_KC & BC_K \\ B_KC & A_K \end{bmatrix},\ \phi_{cl}(x_{cl}) := \phi(x),\ B_{w,cl} := J = [I_2, 0_{2\times n_K}]^T\,, \tag{18}$$

and where the controller dynamics are

$$\left\{\begin{array}{rcl} \dot{x}_K &=& A_Kx_K + B_Ky, \quad x_K \in \mathbb{R}^{n_K} \\ u &=& C_Kx_K + D_Ky \end{array}\right. . \tag{19}$$

We exclude high-gain feedback in the high-frequency range by adding a constraint on the complementary sensitivity function $\|WT\|_\infty \le 1$, where W is a high-pass weighting filter $W(s) := (1\text{e}06s^2 + 1\text{e}04s + 24.99)/(s^2 + 10000s + 2.5\text{e}07)$.

Program (16) was solved for controller orders: 0, 1 and 3. All controllers achieve nearly the same Kreiss norm of 1.005, but differ in terms of the remaining performance/robustness constraints. This is seen by plotting transient amplifications versus time in Fig. 2. Peak values $\mathcal{M}_0(J^T(sI - A_{cl})^{-1}J)$ are all close to 1.10 with $\|J^TJ\| = 1$ as lower bound, see Proposition 2.

The static controller $K = -0.20$ gives a spectral abscissa of $\alpha(A_{cl}) = -1.9899\text{e-}04$ with badly damped modes and a strong roll-off violation of $\|WT\|_\infty = 20.03$. The 1st-order controller $K(s) = (0.001071s - 2.247)/s + 1.483)$ meets the roll-off constraint and achieves a decay rate constraints $\alpha(A_{cl}) = -0.393$. As expected, the 3rd-order controller $K(s) = (-0.008068s^3 - 6.391s^2 + 83.2s - 1673)/(s^3 + 27.97s^2 + 252.8s + 1333)$ provides the best results in terms of decay rate $\alpha(A_{cl}) = -0.811$.

Simulations in closed loop for identical initial conditions are given in Fig. 3. Controllers are switched on at $t = 50$ seconds when the limit cycle is well engaged. The static controller leads to a spiral trajectory barely converging to the origin, a stint which is overcome by increasing the controller order.

Global stability of the origin is established in appendix A.

5.2. **Study of fourth-order dynamics with $4D$ periodic orbit attractor.** The fourth-order model of Brunton and Noack is described as

$$\left\{\begin{array}{rcl} \dot{x} &=& Ax + B_ww + Bu \\ w &=& \phi(x) \\ y &=& Cx \end{array}\right. , \tag{20}$$

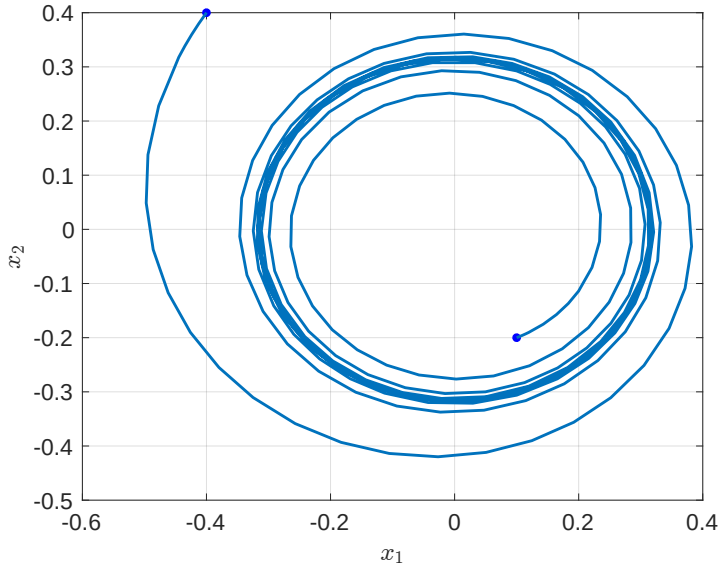

FIGURE 1. Limit cycle attractor of Brunton and Noack model

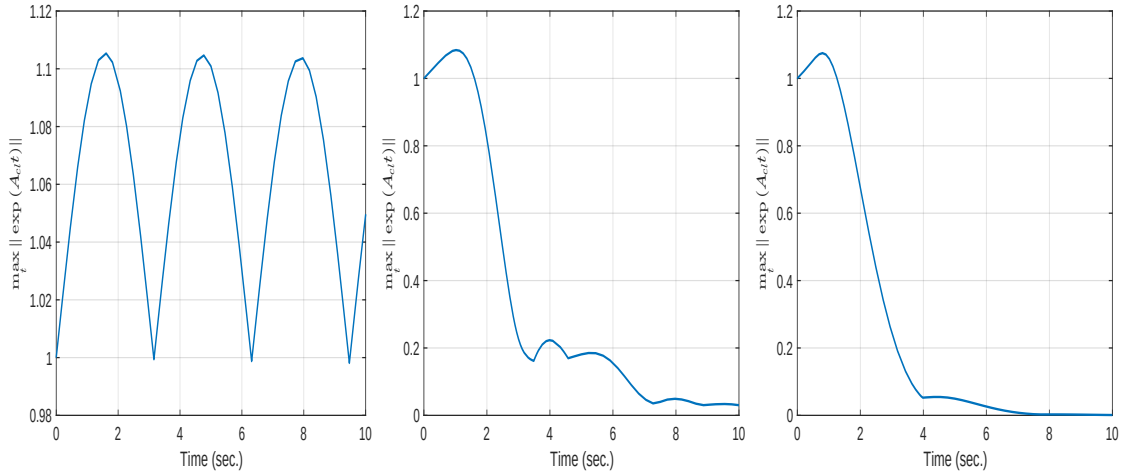

FIGURE 2. From left to right, time evolution of transient amplification for static, 1st-order and 3rd-order controller

with

$$\phi(x) := (\alpha_u(x_1^2 + x_2^2)A_5 + \alpha_a(x_3^2 + x_4^2)A_6))x$$

where

$$A := \operatorname{diag}\left(\begin{bmatrix}\sigma_u & -\omega_u \\ \omega_u & \sigma_u\end{bmatrix}, \begin{bmatrix}\sigma_a & -\omega_a \\ \omega_a & \sigma_a\end{bmatrix}\right),\ B_w := I,\ B := [0\ g\ 0\ g]^T,\ C := [1\ 0\ 1\ 0],$$

$$A_5 := \operatorname{diag}\left(\begin{bmatrix}-\beta_{uu} & -\gamma_{uu} \\ \gamma_{uu} & -\beta_{uu}\end{bmatrix}, \begin{bmatrix}-\beta_{au} & -\gamma_{au} \\ \gamma_{au} & -\beta_{au}\end{bmatrix}\right),\ A_6 := \operatorname{diag}\left(\begin{bmatrix}-\beta_{ua} & -\gamma_{ua} \\ \gamma_{ua} & -\beta_{ua}\end{bmatrix}, \begin{bmatrix}-\beta_{aa} & -\gamma_{aa} \\ \gamma_{aa} & -\beta_{aa}\end{bmatrix}\right),$$

with data given in [14]. The open-loop dynamics are characterized by an unstable fixed point at the origin and an attractive $4D$ periodic orbit. A 1st-order controller is computed to minimize the Kreiss norm as in program (16). The roll-off filter W is unchanged. The optimal controller $K(s) := (0.03538s - 0.5306)/(s + 0.667)$ achieves a Kreiss norm of 1.004 with decay rate and roll-off constraints all met.

Despite the apparent complexity of the dynamics, experience shows that it is possible to bring points of the periodic orbit back to the origin with a fairly large class of *linear* controllers. As an instance, a controller designed using a mixed-sensitivity approach

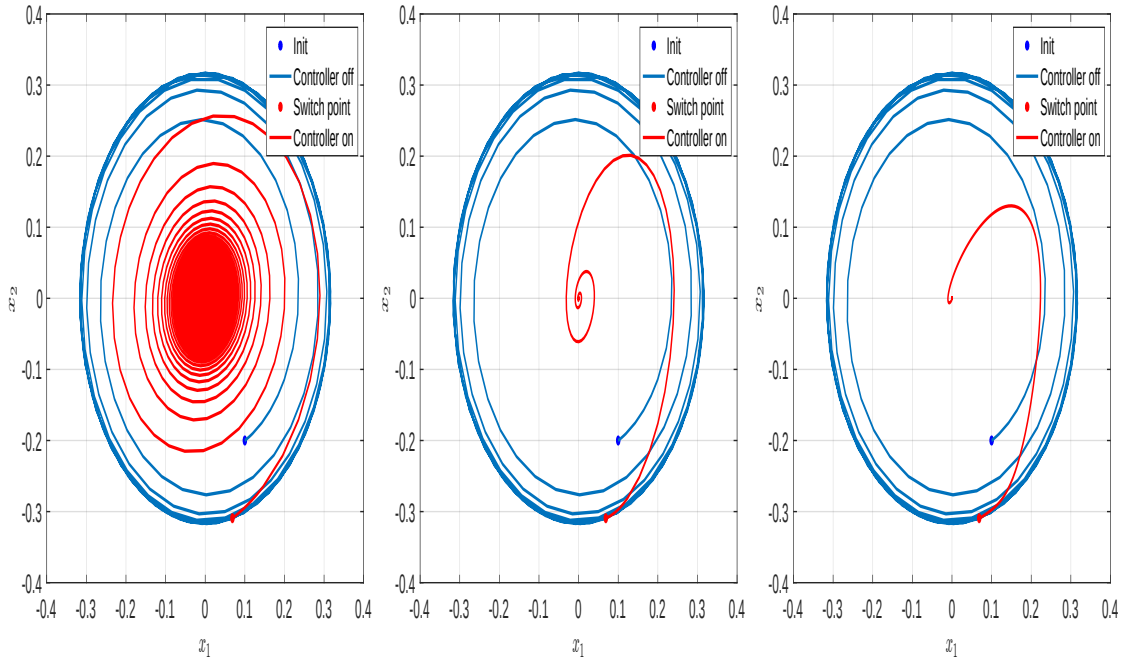

FIGURE 3. From left to right, closed-loop free responses for static, 1st-order and 3rd-order controller

[51, p. 141] with weight $W_1 := \frac{0.001s+5}{s+0.05}$ for S and W as above for T also drives points from the periodic orbit to the origin. A 1st-order controller of this type was obtained as $K(s) := (34.31s+168.1)/(s+32.47)$ with a closed-loop Kreiss constant of 1.54. Simulations show that closed-loop trajectories undergo large deviations before heading back to the origin. See Fig. 4. This remains risky, as attractors when still present may capture trajectories. The controller based on the Kreiss norm corrects such undesirable transients as corroborated in Figs. 4 and 5, where worst-case transients have been plotted. Finally, all controllers globally stabilize the origin and this can be established as was done for the 2nd-order system in appendix A.

6. Applications to nonlinear dynamics with chaos and fixed points

In this section, we consider suppression of undesirable nonlinear regimes such as chaos and fixed points for the Lorenz model.

6.1. **Study of the Lorenz system with chaotic attractor.**

The Lorenz system [31] has three coupled first-order nonlinear differential equations

$$\left\{\begin{array}{rcl} \dot{x}_1 &=& p(x_2 - x_1) \\ \dot{x}_2 &=& Rx_1 - x_2 - x_1x_3 \\ \dot{x}_3 &=& -bx_3 + x_1x_2\,, \end{array}\right. \tag{21}$$

where p, R, and b are given parameters. In this study, we will use $p = 10$ and $b = 1$, while R will be varied to illustrate different nonlinear asymptotic regimes. To begin with, we take $R = 28$, where the Lorenz model has three unstable fixed points with coordinates

$$(0,0,0),\ (\sqrt{R-1}, \sqrt{R-1}, R-1),\ (-\sqrt{R-1}, -\sqrt{R-1}, R-1)\,. \tag{22}$$

For any initial condition $x(0) = x_0$, a repelling effect of these fixed points is observed and trajectories are quickly captured by a chaotic attractor of double-scroll type, shown in Fig. 6.

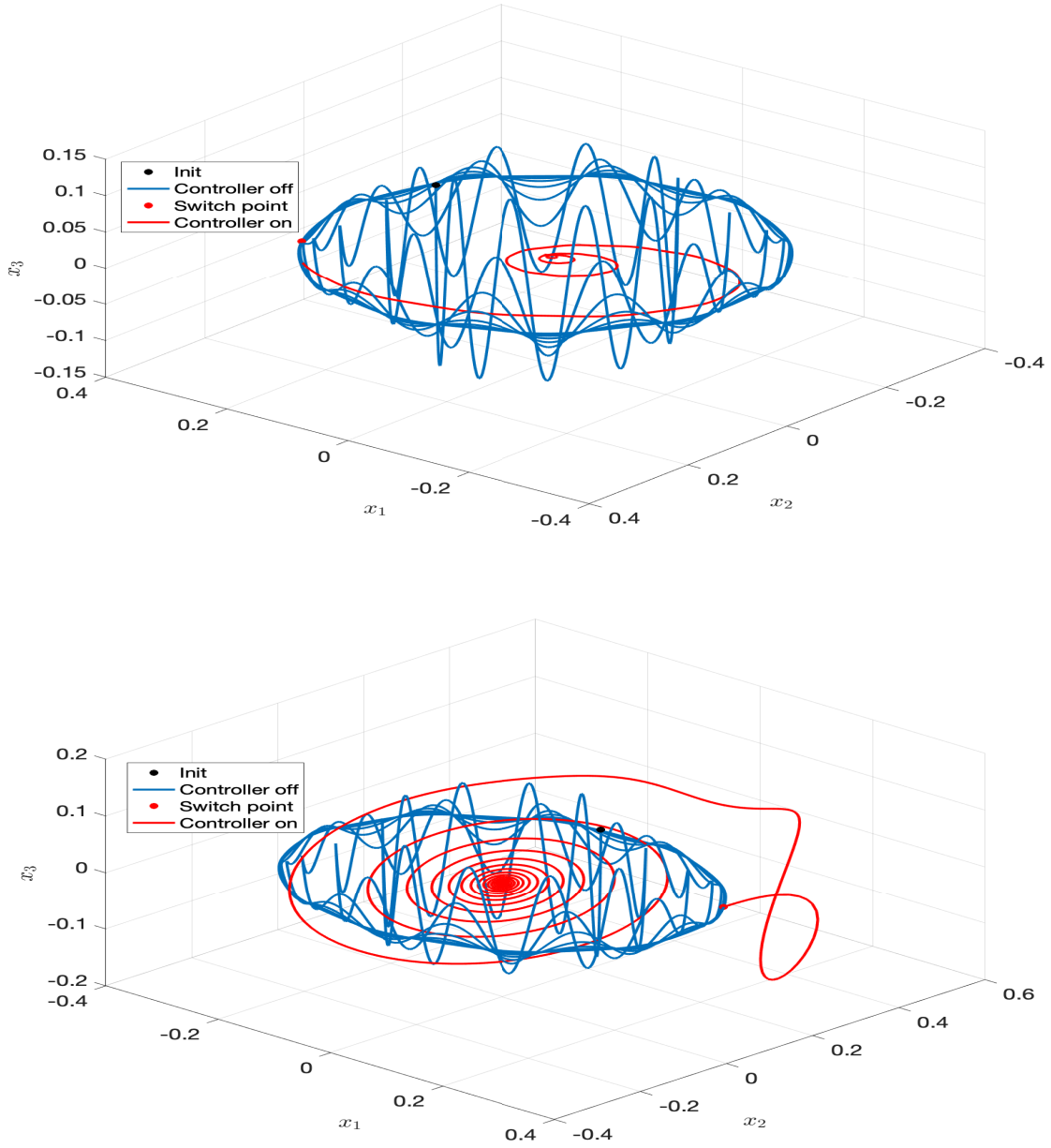

FIGURE 4. Brunton and Noack model. Free open- and closed-loop responses projected in (x_1, x_2, x_3)-space with 1st-order controllers. Top: Kreiss controller. Bottom: mixed-sensitivity controller.

Our feedback goal is therefore suppression of the chaotic attractor and stabilization of the origin through various feedback control strategies. We complement (21) by adding actuation and sensing, letting $B = [0,\ 1,\ 0]^T$ and discussing several cases C, where (A, B, C) is stabilizable and detectable. The Lorenz model is then rewritten as

$$\left\{ \begin{array}{rcl} \dot{x} & = & Ax + B_w w + Bu \\ w & = & \phi(x) \\ y & = & Cx\,, \end{array} \right. \tag{23}$$

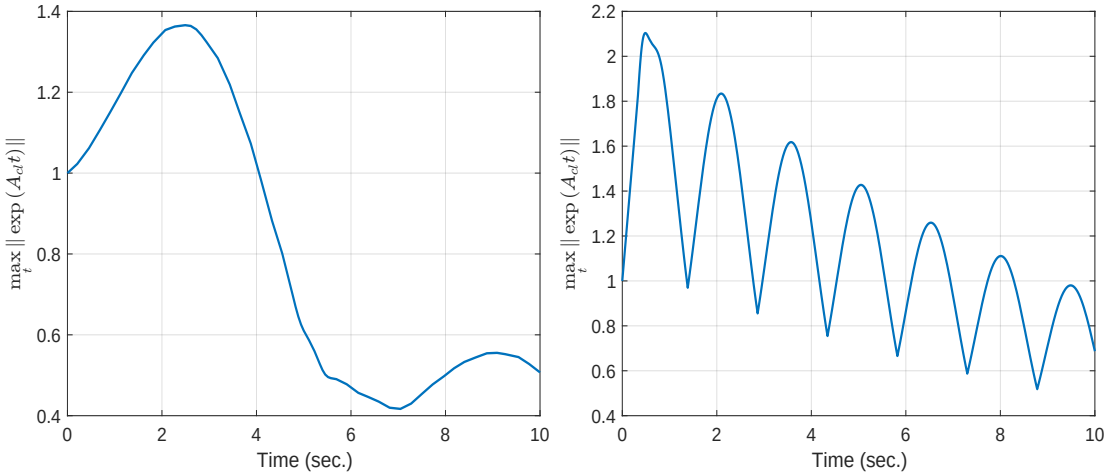

FIGURE 5. Brunton and Noack model. Transient amplifications. Left: Kreiss controller. Right: mixed-sensitivity controller.

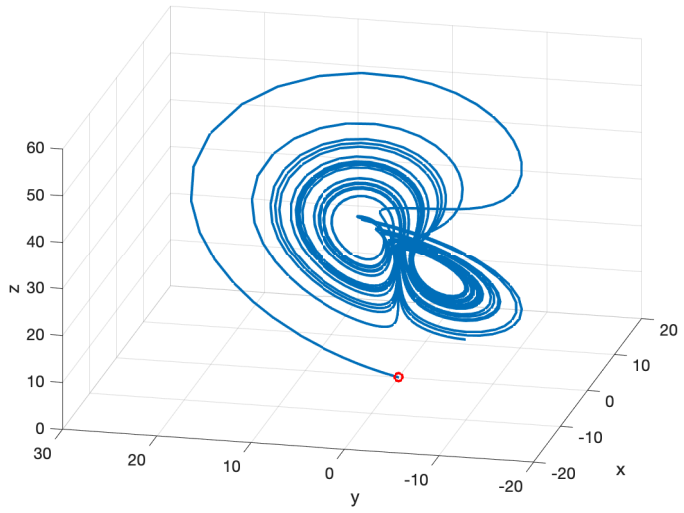

FIGURE 6. Double-Scroll chaotic attractor of the Lorenz model

where u is the control input, y the measurement output. Matrix A collects the linear terms in (21), $\phi(x) := [-x_1x_3,\ x_1x_2]^T$ the nonlinearity, and $B_w := [0_{2\times 1}, I_2]^T$. As observed before, the origin is unstable in the absence of feedback.

When a linear feedback controller $u = K(s)y$ is used with

$$\left\{\begin{array}{rcl} \dot{x}_K &=& A_K x_K + B_K y, \quad x_K \in \mathbb{R}^{n_K} \\ u &=& C_K x_K + D_K y\,, \end{array}\right. \tag{24}$$

the Lorenz model in closed loop becomes:

$$\dot{x}_{cl} \;=\; A_{cl}x_{cl} + B_{w,cl}\phi_{cl}(x_{cl}), \quad x_{cl} := [x^T, x_K^T]^T\,, \tag{25}$$

where

$$A_{cl} := \begin{bmatrix} A + BD_KC & BC_K \\ B_KC & A_K \end{bmatrix},\ \phi_{cl}(x_{cl}) := \phi(x),\ B_{w,cl} := [0_{2\times 1}, I_2, 0_{2\times n_K}]^T\,. \tag{26}$$

6.1.1. *Chaos dynamics: design with the QC approach.* Here we assess the stability properties of the closed loop (25) using the Lyapunov Quadratic Constraints (QC) approach of [36, 24, 30].

A particularity of the Lorenz system is the so-called *lossless property*

$$x_{cl}^T B_{w,cl} w = 0 \text{ for all } x_{cl}, w = \phi(x)\,, \tag{27}$$

which holds globally in state space. The QC approach to stability analysis now relies on the existence of a Lyapunov function $V(x_{cl}) = x_{cl}^T X_{cl} x_{cl}$, with X_{cl} a positive definite matrix, such that

$$\dot{V}(x_{cl}) \leq -\epsilon V(x_{cl}), \epsilon > 0$$

for all x_{cl}, w such that the quadratic constraint in (27), when disregarding $w = \phi(x)$, holds. This is clearly a sufficient possibly conservative condition because of the chosen quadratic in $V(x_{cl})$, and also because the specific dependence of w on the states x is ignored. Using a S-procedure argument [24, 12] to aggregate the lossless constraint (27), this is rewritten as

$$\dot{V}(x_{cl}) + \mu_0 x_{cl}^T B_{w,cl} w \leq -\epsilon V(x_{cl})$$

for all x_{cl}, w, where μ_0 is a S-procedure parameter (sometimes called a Lagrange multiplier), which here is unsigned, as the constraint (27) is an equality. The following equivalent matrix inequality constraints are obtained:

$$\begin{bmatrix} A_{cl}^T X_{cl} + X_{cl} A_{cl} + \epsilon X_{cl} & X_{cl} B_{w,cl} + \mu_0 B_{w,cl} \\ B_{w,cl}^T X_{cl} + \mu_0 B_{w,cl}^T & 0 \end{bmatrix} \preceq 0,\ X_{cl} \succ 0\,. \tag{28}$$

We have the following:

Theorem 5. *There exist a linear time-invariant controller* (24) *such that the sufficient global stability conditions* (28) *hold, if and only if there exist solutions* $X = X^T$ *and* $Y = Y^T$ *in* $\mathbb{R}^{(n-n_\phi)\times(n-n_\phi)}$ *to the following LMIs:*

$$\begin{aligned} N_C^T \left(A^T \begin{bmatrix} X & 0 \\ 0 & I \end{bmatrix} + \begin{bmatrix} X & 0 \\ 0 & I \end{bmatrix} A + \epsilon \begin{bmatrix} X & 0 \\ 0 & I \end{bmatrix} \right) N_C \prec 0 \\ N_B^T \left(A \begin{bmatrix} Y & 0 \\ 0 & I \end{bmatrix} + \begin{bmatrix} Y & 0 \\ 0 & I \end{bmatrix} A^T + \epsilon \begin{bmatrix} Y & 0 \\ 0 & I \end{bmatrix} \right) N_B \prec 0 \\ \begin{bmatrix} X & 0 & I & 0 \\ 0 & I & 0 & I \\ I & 0 & Y & 0 \\ 0 & I & 0 & I \end{bmatrix} \succeq 0\,, \end{aligned} \tag{29}$$

where N_C *and* N_B *are bases of the null space of* C *and* B^T*, respectively.*

Moreover, the controller order is determined by the rank of $I_{n-n_\phi} - XY$ *with* n_ϕ *the vector dimension of the nonlinearity.*

Proof: See appendix B.

Note that Theorem 5 applies to any nonlinear system with similar structure for which (27) holds.

For the Lorenz model, we have a loss of rank of at least $n_\phi = 2$, the vector dimension of the nonlinearity. For the QC approach this means that controllers can have order at most $n - n_\phi = 1$. For problems with nonlinearity of dimension n, the plant order, only static output feedback controllers can be computed. In that case the BMI (37) reduces to the LMI feasibility problem:

$$(A + BKC)^T + (A + BKC) \prec 0\,,$$

or equivalently, to minimization of the numerical abscissa $\omega(A + BKC)$, defined as $\omega(M) := 1/2\lambda_{\max}(M + M^T)$. This is in line with the results in [24] for transitional flow studies. On the other end, when $n_\phi = 0$, the plant is linear and the controller can

be of full order. The last step is construction of the controller given X and Y from (29), which is standard and found in [20].

Application to the Lorenz model with x-measurement, yields a 1st-order controller $K(s) = -(306.5 + 2809)/(s + 0.1044)$. Simulation in closed loop is shown in Fig. 7 (top left corner). The feedback controller is switched on after 15 seconds, when the chaotic regime is well engaged.

Characterization of state-feedback controllers is easily derived from the second projection LMI in (29), or using $u = Kx$ and $C = I$ in the BMI (28):

$$(A + BK)^T \operatorname{diag}(X, I) + (.)^T \prec -\epsilon \operatorname{diag}(X, I),\ X \succ 0\,, \tag{30}$$

or equivalently, using a congruence transformation $\operatorname{diag}(Y, I) = \operatorname{diag}(X, I)^{-1}$, on the left- and right-hand sides of the first matrix inequality in (30)

$$(A + BK) \operatorname{diag}(Y, I) + (.)^T \prec -\epsilon \operatorname{diag}(Y, I),\ Y \succ 0\,. \tag{31}$$

The constraint (31) is turned into an LMI feasibility program using the standard change of variable $W := K \operatorname{diag}(Y, I)$:

$$A \operatorname{diag}(Y, I) + BW + (.)^T \prec -\epsilon \operatorname{diag}(Y, I),\ Y \succ 0\,. \tag{32}$$

All LMI characterizations derived so far can be solved by standard convex SDP software as *LMILab* [33] or *SeDuMi* [42]. Solving (32) for the Lorenz model yields a globally stabilizing state-feedback controller $K = W \operatorname{diag}(P_{11}, I) = [-154, 400.245, 0]$. A simulation is shown in Fig. 7 top right.

The fact that the state-feedback controller does not use the z-measurement suggests that even simpler controller structures should be satisfactory, e.g. using static output feedback in x or y. For x-measurement alone, we have $C = [1, 0, 0]$ and the BMI characterization is the same as in (30) with $A + BKC$ replacing $A + BK$. For a scalar K this is easily solved by sweeping an interval of K values and solving for the resulting LMIs with K fixed. We obtain $K = -27.01$ with search interval $[-100, 100]$. Simulations are displayed in Fig. 7, bottom left.

Similar results can be obtained with y-measurement feedback alone. The gain value is $K = -27.01$, and simulations are given in Fig. 7, bottom right.

6.1.2. *Chaos dynamics: Kreiss norm minimization.* We now investigate whether similar results can be achieved with controllers minimizing the Kreiss system norm. Here we follow a different strategy which is to decouple the linear dynamics $\dot{x} = Ax$ from the nonlinearity ϕ by way of mitigating transients due to initial conditions or L^1 disturbances. While this is a heuristic in the first place, it can of course in a second step be certified rigorously using the same QC approach, now for analysis. This has the advantage that BMIs are replaced by LMIs. In addition, the technique is applicable in a much more general context beyond the Lorenz model as seen in sections 5.1 and 5.2 when the QC approach turns out too conservative.

Controllers based on minimizing the Kreiss norm alone are computed through the following min-max program

$$\begin{array}{ll} \text{minimize} & \max\limits_{\delta\in[-1,1]} \left\| J^T \left(sI - \left(\frac{1-\delta}{1+\delta} A_{cl}(K) - I\right)\right)^{-1} J \right\|_\infty \\ \text{subject to} & K \text{ robustly stabilizing, } K \in \mathscr{K}\,, \end{array} \tag{33}$$

with the definitions already given for program (16).

Program (33) was solved for four controller structures: x-measurement dynamic output feedback, full state feedback, static x-measurement feedback, and static y-measurement feedback. Controller gains were computed as $K(s) = -(47.06s + 715.7)/(s + 17.95)$, $[-41.07, -13.78, 0]$, -34.70 and -32.55, respectively. In each case a Kreiss constant of

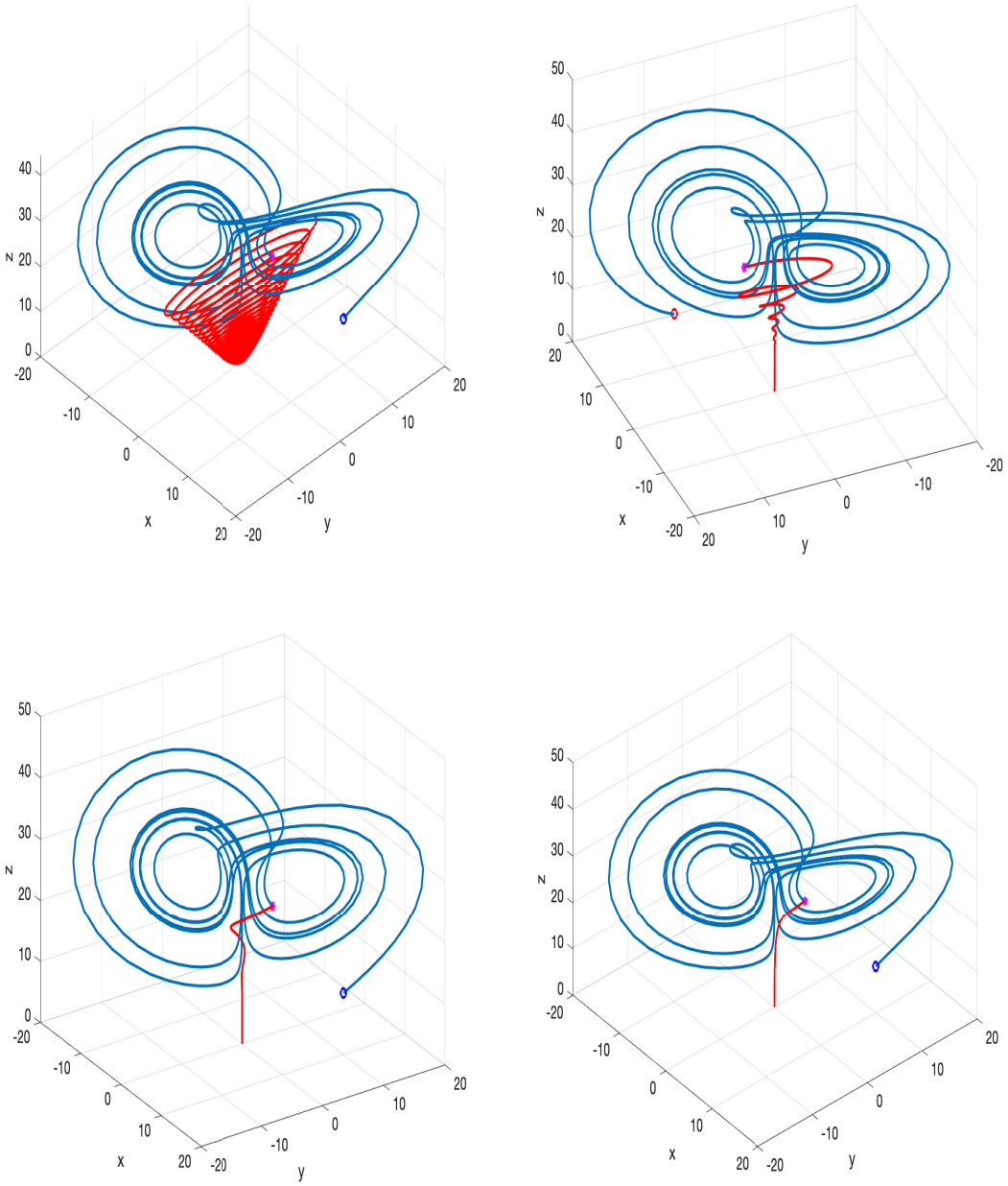

FIGURE 7. Suppression of Lorenz double-scroll chaotic attractor using QC approach
Top left: x-measurement dynamic feedback, Top right: state feedback
Bottom left: : x-measurement static feedback, Bottom right: : y-measurement static feedback
Open loop: blue curve, Closed loop: red curve.

unit value with $\mathcal{M}_0(G) = 1$ was achieved, meaning that the linear dynamics do no longer amplify transients in the Lorenz model. Note that unlike the matrix case, $\mathcal{M}_0(G) = 1$ cannot be inferred directly from $\mathcal{K}(G) = 1$, but can be certified a posteriori. Naturally, all controllers have been tested for global stability of the Lorenz model, which for K fixed uses the characterization in (28) and requires solving a convex SDP. Simulations are given in Fig. 8.

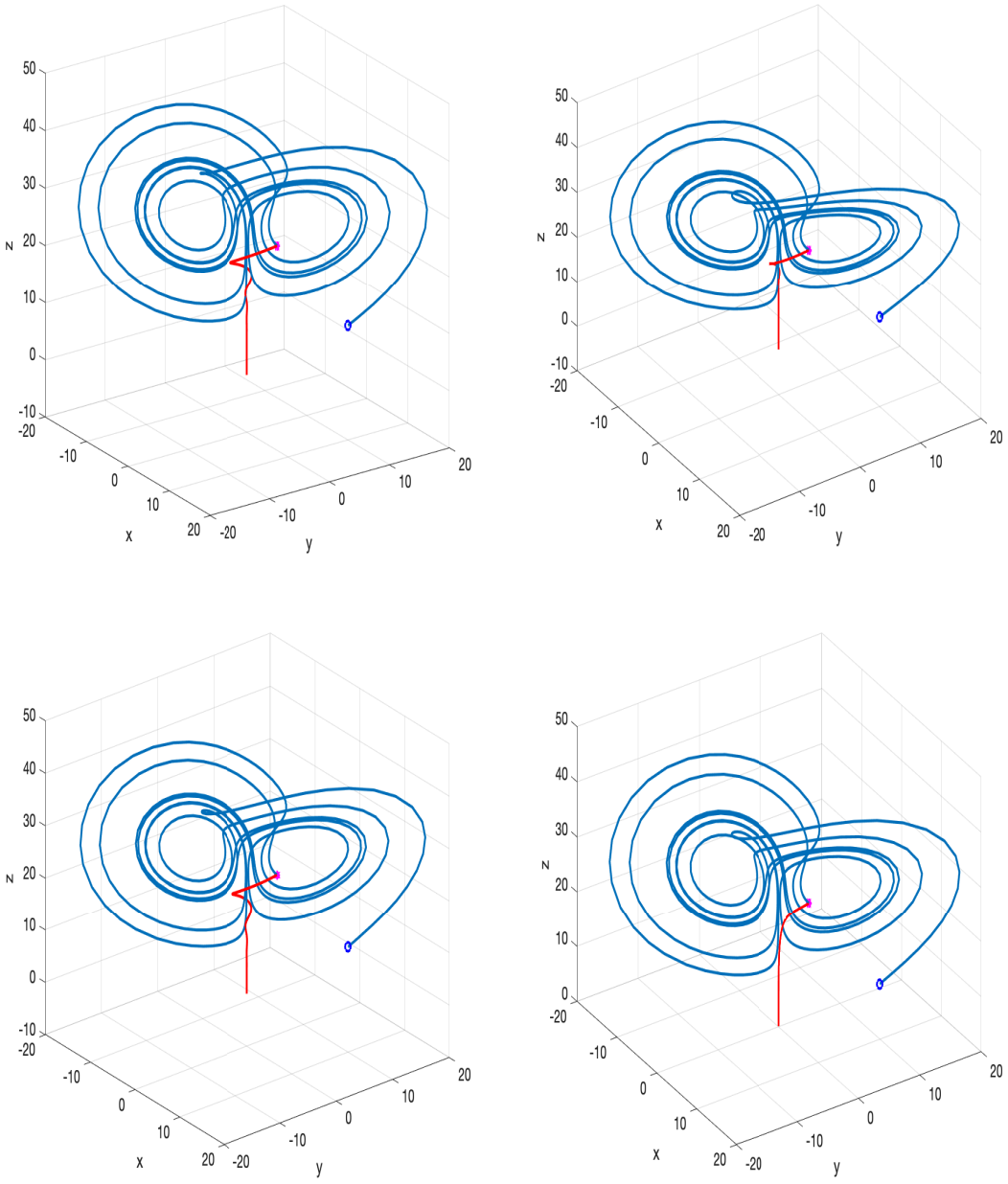

FIGURE 8. Suppression of Lorenz chaotic attractor using Kreiss norm minimization
Top left: x-measurement dynamic feedback, Top right: state feedback
Bottom left: : x-measurement static feedback, Bottom right: : y-measurement static feedback
Open loop: blue curve, Closed loop: red curve.

6.2. **Study of the Lorenz system with fixed points.** For $R < 1$, the origin is the only stable equilibrium of (21) and the Lorenz model is then globally stable. When the Lorenz parameter is chosen as $1 < R < 17.5$, the chaotic attractor disappears and is replaced with stable fixed points. For instance, when $R = 10$, the Lorenz model has an unstable fixed point at the origin and two stable fixed points given in (22). A typical illustration of that situation is shown in Fig. 9. Trajectories with initial conditions arbitrarily close to 0 are quickly captured by one of the fixed points.

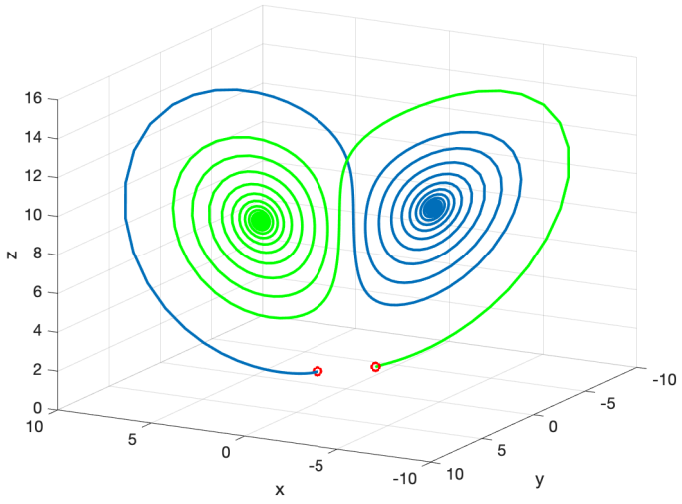

FIGURE 9. Lorenz model for $1 < R < 17.5$
Unstable origin and two stable fixed points

Despite this quite different pattern of the attracting regime, synthesis proceeds along similar lines as in section 6.1. We remove the undesirable fixed points and stabilize the origin globally using static state-feedback, and dynamic and static output-feedback, comparing QC approach and Kreiss norm minimization.

6.2.1. *Fixed-point dynamics: design with the QC approach.* As before, we start with the QC approach. A state-feedback controller was computed as $K = [-136.40, 0.24, 0]$. Again the z measurement is not used. That leads us to computing static output feedback controllers given as $K = -9.01$ and $K = -9.01$ for the x and y measurements alone, respectively. A dynamic 1st-order x-measurement output feedback controller was computed as $K = -(288.5s + 2807)/(s + 0.104)$ based on Theorem 5. All computed controllers globally stabilize the origin. This is illustrated in Fig. 10 for two initial conditions.

6.2.2. *Fixed-point dynamics: Kreiss system norm.* Controllers with identical structure were computed using Kreiss norm minimization. Dynamic 1st-order x-measurement output feedback, full state, x-measurement and y-measurement static feedback were obtained as $K = -(12.23s + 67.63)/(s + 5.541)$, $K = [-4.47, -6.92, 0]$, $K = -26.32$ and $K = -11.53$, respectively. All controllers were certified to stabilize the origin globally through feasibility of the LMI (28). Simulations are shown in Fig. 11 and should be compared to Fig. 10.

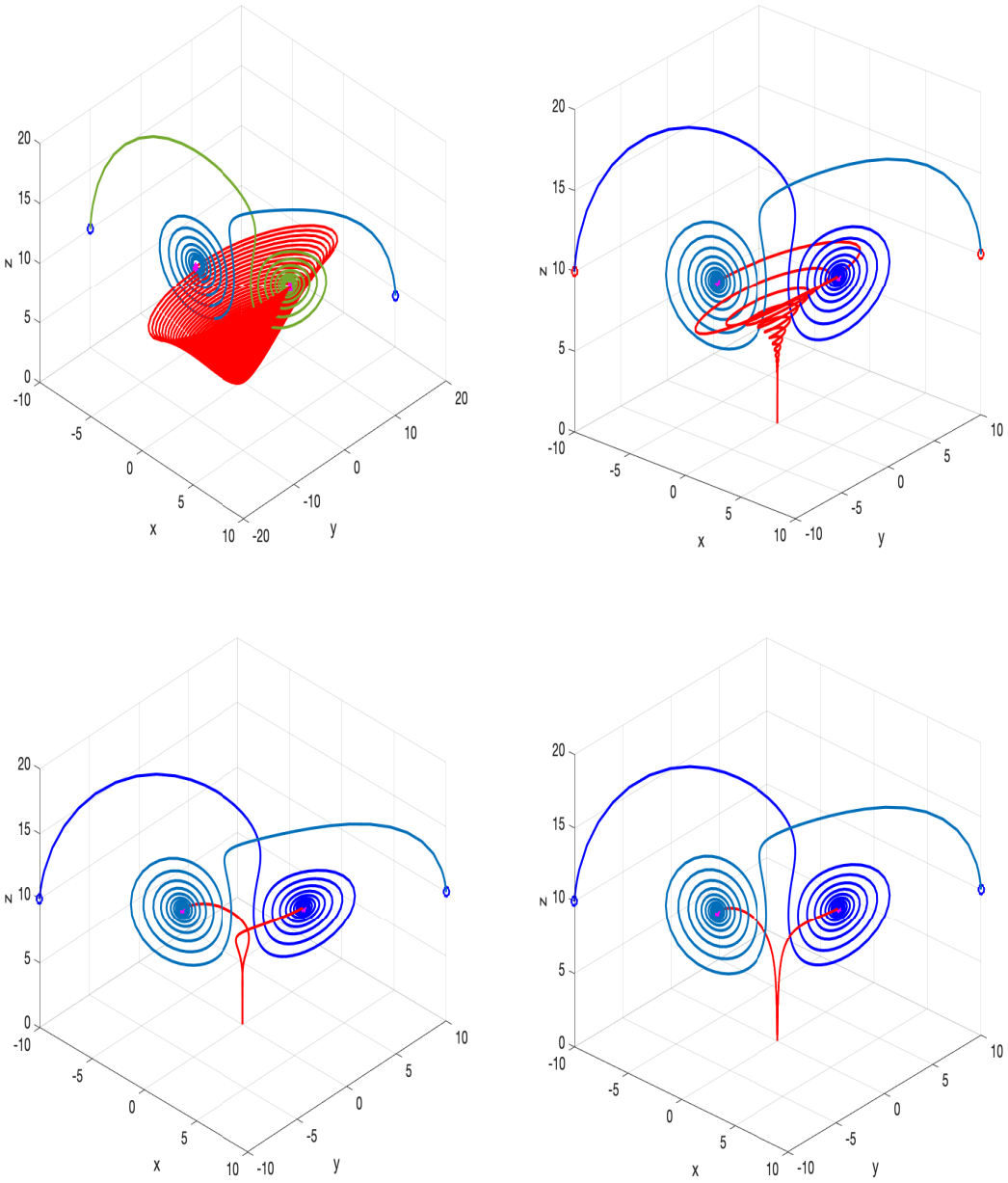

FIGURE 10. Suppression of fixed point attractors using QC approach
Top left: x-measurement dynamic feedback, Top right: state feedback
Bottom left: : x-measurement static feedback, Bottom right: : y-measurement static feedback
Open loop: blue curve, Closed loop: red curve.

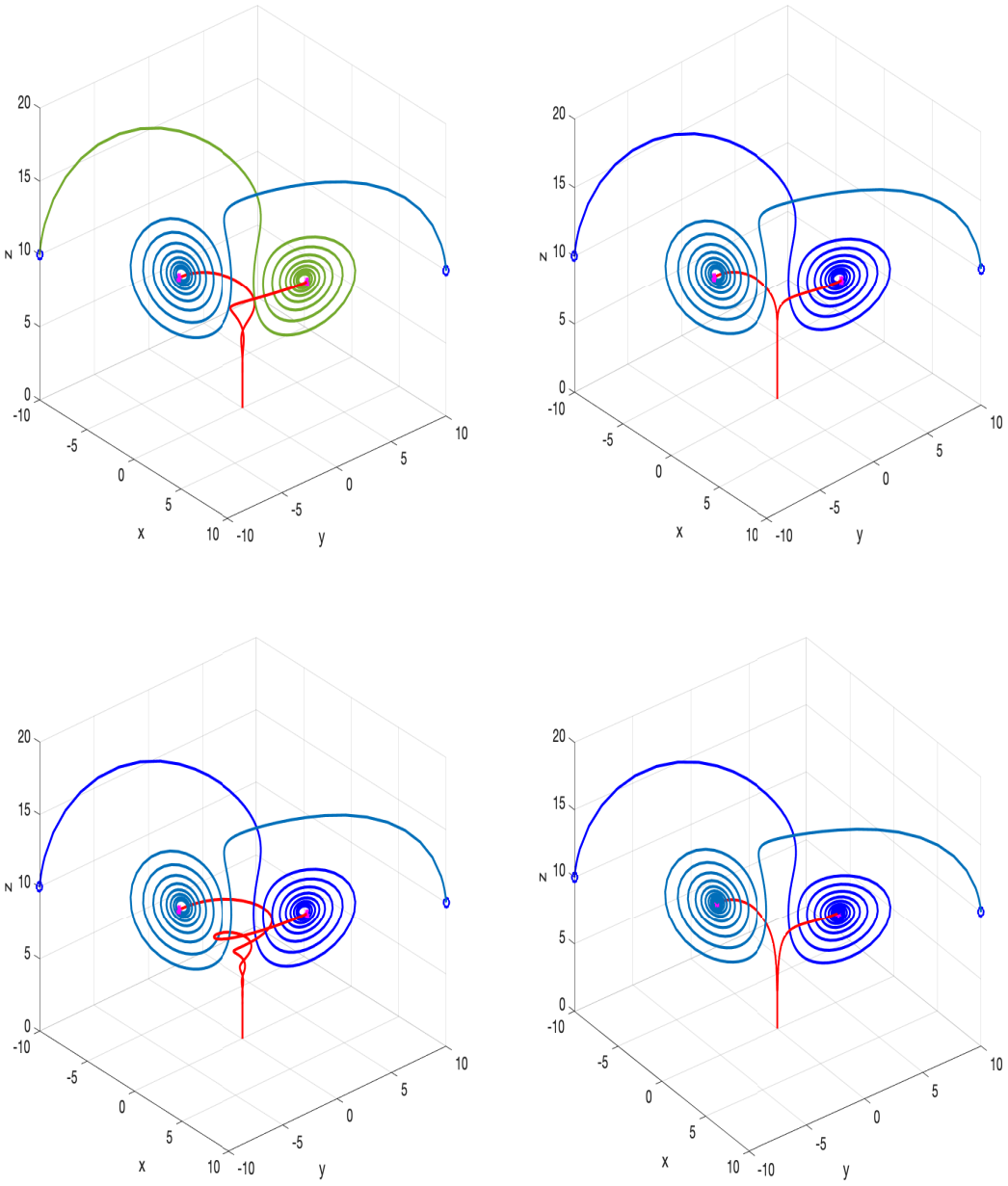

FIGURE 11. Suppression of fixed point attractors using Kreiss norm minimization
Top left: x-measurement dynamic feedback, Top right: state feedback
Bottom left: : x-measurement static feedback, Bottom right: : y-measurement static feedback
Open loop: blue curve, Closed loop: red curve.

7. Conclusion

The idea to stabilize nonlinear systems in closed loop by mitigating transients of the linearized closed loop was investigated, the rationale being that large transients are responsible for driving the nonlinear dynamics outside the region of local stability. Heuristic approaches tailored to transients caused by noise, persistent perturbations, and finite consumption disturbances were obtained, opening up new possibilities for analysis and control of linear and nonlinear systems.

The time-domain worst case transient peak norm $\mathcal{M}_0(G)$ was identified as suitable to assess transients caused by L_1-disturbances. The Kreiss system norm $\mathcal{K}(G)$ was introduced and studied as a frequency domain approximation of $\mathcal{M}_0(G)$, better suited for the purpose of optimization due to its representation as a parametric robust control problem. In our numerical testing, Kreiss norm optimization was evaluated by matching it, in small to medium size cases where possible, with a properly extended QC approach.

Future work may strive to enable Kreiss norm minimization for large-dimensional plants, such as realistic fluid flow. This is challenging, but may be within reach when model sparsity is exploited, and specialized linear algebra is used. In contrast, LMI techniques and SOS certificates are no longer in business for such large scales.

Appendix A

We consider the closed-loop system (15) in polar coordinates

$$\begin{aligned}\dot r &= \sigma r - \alpha\beta r^3 + gKr\sin^2\phi\\ \dot\phi &= \omega + \alpha\gamma r^2 + gK\cos\phi\sin\phi\end{aligned}\tag{34}$$

First observe that $r(t)$ must be bounded. Indeed, we have $\dot r \le 0$ for

$$r^2 \ge \frac{\sigma + gK\sin^2\phi}{\alpha\beta}$$

which due to $K<0$ means that states r with

$$r^2 > \frac{\sigma}{\alpha\beta} =: r_0^2$$

cannot be reached (from below). Namely if $r(0)<r_0$, then the trajectory may never reach values $r(t)>r_0$, as this would require derivatives $\dot r>0$ in between r_0 and $r(t)>r_0$. Even when $r(0)>r_0$, then $\dot r<0$ on some $[0,\epsilon)$, so the trajectory decreases until $r(t)=r_0$ is reached, and then the previous argument shows that it cannot rebounce to values $>r_0$. In conclusion, the trajectories of the system are bounded.

Let us look for steady states (x^*,y^*). In the original (x,y)-system we have (with $r^2=x^2+y^2$)

$$\begin{aligned}0 &= (\sigma-\alpha\beta r^2)x - \omega y - \alpha\gamma r^2 y\\ 0 &= \omega x + \alpha\gamma r^2 x + \sigma y - \alpha\beta r^2 y + gKy\end{aligned}$$

and this can be written

$$A(r) := \begin{bmatrix}\sigma-\alpha\beta r^2 & -\omega-\alpha\gamma r^2\\ \omega+\alpha\gamma r^2 & \sigma-\alpha\beta r^2+gK\end{bmatrix}\begin{bmatrix}x\\y\end{bmatrix} = \begin{bmatrix}0\\0\end{bmatrix}$$

For this system to have a non-zero solution $(x^*,y^*)\neq(0,0)$, the determinant of the system matrix $A(r)$ must vanish, which leads to

$$(\sigma-\alpha\beta r^2)^2 + gK(\sigma-\alpha\beta r^2) + (\omega+\alpha\gamma r^2)^2 = 0.$$

This quadratic equation in $\sigma-\alpha\beta r^2$ has no real solution for $g^2K^2 - 4(\omega+\alpha\gamma r^2)^2 < 0$, which gives the following

Proposition 4. *Suppose $-K < \frac{2\omega}{g}$. Then the only steady state of the closed-loop system is $(0,0)$.*

The origin is locally exponentially stable, so there exists a largest ball $B(0,\rho)$ such that all trajectories starting in $B(0,\rho)$ converge to $(0,0)$. Suppose $\rho<\infty$, then there exists $(x_0,y_0)\notin B(0,\rho)$ such that the trajectory starting at (x_0,y_0) does not enter the ball $B(0,\rho)$. Since it is a bounded trajectory, the Poincaré-Bendixson theorem implies

that it must approach a limit cycle. For a limit cycle to exist, the system must admit a periodic solution.

We therefore look for conditions which allow to exclude the existence of a periodic solution. The Bendixson condition tells that this is the case when $P_x + Q_y$ does not change sign, where P, Q are the right hand sides of (15) with the loop $u = Ky$ closed. We get

$$P_x + Q_y = 2\sigma - 4\alpha\beta r^2 + gK$$

and this has negative sign for $K < -\frac{2\sigma}{g}$. We conclude the

Proposition 5. *Suppose $K \in \mathbb{R}$ satisfies $K < -\frac{2\sigma}{g}$ and $-K < \frac{2\omega}{g}$. Then (15) is globally stabilized by the static controller $u = Ky$.*

A.1. **Dynamic controllers.** Consider the case of dynamic controllers. Closed-loop dynamics are obtained as follows ($r^2 = x^2 + y^2$):

$$\begin{bmatrix} \dot{x} \\ \dot{y} \\ \dot{x}_K \end{bmatrix} = \begin{bmatrix} (\sigma - \alpha\beta r^2) & -(\omega + \alpha r^2\gamma) & 0 \\ (\omega + \alpha\gamma r^2) & (\sigma + gD_K - \alpha\beta r^2) & gC_K \\ 0 & B_K & A_K \end{bmatrix} \begin{bmatrix} x \\ y \\ x_K \end{bmatrix} .$$

The equilibrium equations give $x_K = -A_K^{-1}B_K y$, assuming that A_K is invertible. This leads to

$$\begin{bmatrix} (\sigma - \alpha\beta r^2) & (\omega + \alpha r^2\gamma) \\ (\omega + \alpha\gamma r^2) & (\sigma - \alpha\beta r^2 + g(D_K - C_K A_K^{-1} B_K)) \end{bmatrix} \begin{bmatrix} x \\ y \end{bmatrix} = \begin{bmatrix} 0 \\ 0 \end{bmatrix} ,$$

which as before, has $(0, 0)$ as unique solution if and only if the system matrix is invertible. The determinant quadratic equation in $\sigma - \alpha\beta r^2$ has no real solution and is thus non-zero when

$$(g(D_K - C_K A_K^{-1} B_K))^2 - 4(\omega + \alpha\gamma r^2)^2 < 0 \,,$$

which is guaranteed when

$$|D_K - C_K A_K^{-1} B_K| < 2\omega/g \,.$$

Note the latter involves a constraint on the DC gain of the dynamic controller $K(s) = C_K(sI - A_K)^{-1}B_K + D_K$.

The polar form of these differential equations for (x, y) is obtained as

$$\begin{aligned} \dot{r} &= \sigma r - \alpha\beta r^3 + gD_K r \sin^2\phi + gC_K x_K \sin\phi \\ \dot{\phi} &= \omega + \alpha\gamma r^2 + gD_K \cos\phi \sin\phi + gC_K x_K \cos\phi \\ \dot{x}_K &= A_K x_K + B_K r \sin\phi \end{aligned} \tag{35}$$

Assuming that A_K is Hurwitz as is the case for all controllers based on the Kreiss norm, the third equation in (35) gives us on every finite interval $[0, t_0]$ an estimate of the form $\max_{0\le t\le t_0} |x_K(t)| \le c \max_{0\le t\le t_0} r(t)$ for a constant $c > 0$ independent of t_0. Indeed, $x_K(t) = \exp(tA_K)x_0 + \int_0^t \exp((s-t)A_K)B_K \sin\phi(s) r(s) ds$, hence from Young's inequality (with $q = r = \infty$, $p = 1$), we get

$$\max_{0\le t\le t_0} |x_K(t)| \le c_1 + \|B_K\| \| \exp(tA_K)\|_1 \max_{0\le t\le t_0} r(t) \le c_1 + c_2 \max_{0\le t\le t_0} r(t) \le c \max_{0\le t\le t_0} r(t).$$

Therefore by the comparison theorem, (see Lemma 7 below), applied to the first equation in (35), $r(t)$ is bounded above by the solution of the equation $\dot{r} = (\sigma + g|D_K| + g\|C_K\|c)r - \alpha\beta r^3$. The latter, however, is globally bounded, as the negative term $-\alpha\beta r^3$ dominates for large $r > 0$. Having established global boundedness of $r(t)$, we go back into the equation $\dot{x}_K = A_K x_K + B_K r \sin\phi$, from which we now derive global boundedness of x_K, and so altogether trajectories of (35) remain bounded.

Lemma 7. (See e.g. [50, Thm. 2.1, p. 93]). *Suppose ϕ satisfies $|\phi(t,x)-\phi(t,x')| \leq M|x-x'|$ for all $t \in [t_0,t_1]$ and x, x', and is jointly continuous. Let $v(t)$ be an absolutely continuous function such that $\dot{v}(t) \leq \phi(t,v(t))$ for almost all $t \in [t_0,t_1]$. Then $v(t) \leq u(t)$ on $[t_0,t_1]$, where $u(t)$ is the solution of $\dot{u}(t) = \phi(t,u(t))$ with initial value $u(t_0)$ satisfying $v(t_0) \leq u(t_0)$.* □

We are now in the situation addressed in [49, Corollary], which says that if a C^1-function $V(x)$ can be found satisfying

$$\dot{V}(x) + \ddot{V}(x) \neq 0 \text{ for all } x \neq 0 \tag{36}$$

then trajectories either converge $x(t) \to 0$, or escape to infinity $|x(t)| \to \infty$. Since we have already ruled out the latter, we have then a certificate of global asymptotic stability. For this model, we have used the more restrictive condition $\dot{V}(x) < 0$, with $V(x) = V_1(x) + \dot{V}_2(x)$ and V_1, V_2 are chosen as multivariate polynomials. See [1] for details. The polynomials are then sought using *sostools* [38].

For both the 1st- and 3rd-order controllers, a solution was obtained with V_1 and V_2 sums of monomials of degree 2. For the simpler 1st-order controller, with $x_{cl} = (x, y, x_K)$ this reads

$$V_1(x_{cl}) = 2.556x^2 - 1.389xy - 0.02803xx_K + 2.897y^2 - 3.846e\text{-}5yx_K + 0.003159x_K^2$$
$$V_2(x_{cl}) = -0.2061x^2 + 0.008941xy - 1.324e\text{-}6xx_K - 0.1787y^2 + 1.641e\text{-}5yx_K - 0.008169x_K^2\,.$$

We have established that $x(t) \to 0$.

Appendix B

Since the first matrix in (28) has a zero principal sub-matrix, the corresponding row and column terms should be zero for this matrix to be negative semi-definite. This leads to $X_{cl}B_{w,cl} + \mu_0 B_{w,cl} = 0$. Also, the $(1,1)$ sub-matrix should be negative semi-definite. Using a partitioning in X_{cl} conformable to that of $B_{w,cl}$ in (26), we have

$$X_{cl} = \begin{bmatrix} X & X_{12} & X_{13} \\ X_{12}^T & X_{22} & X_{23} \\ X_{13}^T & X_{23}^T & X_{33} \end{bmatrix}, \text{ with } X \in \mathbb{R}^{(n-n_\phi)\times(n-n_\phi)},\ X_{22} \in \mathbb{R}^{n_\phi \times n_\phi},\ X_{33} \in \mathbb{R}^{n_K \times n_K}$$

with n_ϕ the vector dimension of the nonlinearity ϕ. This gives $X_{12} = 0$, $X_{22} = -\mu_0 I$ and $X_{23} = 0$. Due to homogeneity of the problem, μ_0 is set to -1, and since X_{22} should be positive definite, we get $X_{22} = I$. Also, non-strict feasibility can be replaced with strict feasibility by reducing ϵ if necessary. Summing up, assessing global stabilization with a dynamic controller $K(s)$ reduces to a specially structured Lyapunov inequality

$$A_{cl}^T X_{cl} + X_{cl}A_{cl} + \epsilon X_{cl} \prec 0,\ \ X_{cl} = \begin{bmatrix} X & 0 & X_{13} \\ 0 & I & 0 \\ X_{13}^T & 0 & X_{33} \end{bmatrix}, X_{cl} \succ 0\,. \tag{37}$$

This is rewritten in the familiar form:

$$\Psi + P^T\Theta Q + Q^T\Theta P \prec 0,\ \ X_{cl} = \begin{bmatrix} X & 0 & X_{13} \\ 0 & I & 0 \\ X_{13}^T & 0 & X_{33} \end{bmatrix}, X_{cl} \succ 0\,, \tag{38}$$

with appropriate matrices Ψ, P, Q depending on X, A, B, C and controller data gathered in

$$\Theta := \begin{bmatrix} A_K & B_K \\ C_K & D_K \end{bmatrix}.$$

We can then apply the Projection Lemma [20] to eliminate Θ, which leads to LMI solvability conditions. There exist controllers of order n_K if and only if $W_P^T \Psi W_P \prec 0$ and $W_Q^T \Psi W_Q \prec 0$, for some $X_{cl} \succ 0$. Introducing the inverse of X_{cl} as

$$Y_{cl} := X_{cl}^{-1} = \begin{bmatrix} Y & 0 & Y_{13} \\ 0 & I & 0 \\ Y_{13}^T & 0 & Y_{33} \end{bmatrix},$$

and following [20], the two projection inequalities are computed as

$$\begin{aligned} N_C^T \left(A^T \begin{bmatrix} X & 0 \\ 0 & I \end{bmatrix} + \begin{bmatrix} X & 0 \\ 0 & I \end{bmatrix} A + \epsilon \begin{bmatrix} X & 0 \\ 0 & I \end{bmatrix} \right) N_C \prec 0 \\ N_B^T \left(A \begin{bmatrix} Y & 0 \\ 0 & I \end{bmatrix} + \begin{bmatrix} Y & 0 \\ 0 & I \end{bmatrix} A^T + \epsilon \begin{bmatrix} Y & 0 \\ 0 & I \end{bmatrix} \right) N_B \prec 0 \end{aligned} \tag{39}$$

where N_C and N_B are bases of the null space of C and B^T, respectively. Also, completion of $X_{cl} = Y_{cl}^{-1} \succ 0$ and $X_{cl} \in \mathbb{R}^{(n+n_K)\times(n+n_K)}$ from X and Y is equivalent to [37, 20]

$$\begin{bmatrix} X & 0 & I & 0 \\ 0 & I & 0 & I \\ I & 0 & Y & 0 \\ 0 & I & 0 & I \end{bmatrix} \succeq 0, \ \operatorname{rank} \left(I_n - \begin{bmatrix} Y & 0 \\ 0 & I_{n_\phi} \end{bmatrix} \begin{bmatrix} X & 0 \\ 0 & I_{n_\phi} \end{bmatrix} \right) \leq n_K \,. \tag{40}$$

Clearly, the maximal rank is $\operatorname{rank}(I - YX) \leq n - n_\phi$ and determines the controller order. Finally, for X and Y solutions to (39) and (40), the full matrix X_{cl} can be reconstructed as well as controller state-space data (A_K, B_K, C_K, D_K) [20].

References

[1] Amir Ali Ahmadi and Pablo A Parrilo. On higher order derivatives of Lyapunov functions. In *Proceedings of the 2011 American Control Conference*, pages 1313–1314. IEEE, 2011.

[2] P. Apkarian, M. N. Dao, and D. Noll. Parametric robust structured control design. *Automatic Control, IEEE Transactions on*, 60(7):1857–1869, 2015.

[3] P. Apkarian and D. Noll. Controller design via nonsmooth multi-directional search. *SIAM J. on Control and Optimization*, 44(6):1923–1949, 2006.

[4] P. Apkarian and D. Noll. Nonsmooth optimization for multiband frequency domain control design. *Automatica*, 43(4):724 – 731, 2007.

[5] Pierre Apkarian and Dominikus Noll. Nonsmooth H_∞ synthesis. *IEEE Transactions on Automatic Control*, 51(1):71–86, 2006.

[6] Pierre Apkarian and Dominikus Noll. Nonsmooth optimization for multidisk H_∞ synthesis. *European Journal of Control*, 12(3):229–244, 2006.

[7] Pierre Apkarian and Dominikus Noll. Worst-case stability and performance with mixed parametric and dynamic uncertainties. *International Journal of Robust and Nonlinear Control*, 27(8):1284–1301, 2017.

[8] Pierre Apkarian and Dominikus Noll. Optimizing the Kreiss constant. *SIAM Journal on Control and Optimization*, 58(6):3342–3362, 2020.

[9] Pierre Apkarian and Dominikus Noll. Mixed L_1/H_∞-synthesis for L_∞-stability. *International Journal of Robust and Nonlinear Control*, 32(4):2119–2142, 2022.

[10] S. Boyd and C. Barratt. *Linear Controller Design: Limits of Performance*. Prentice-Hall, 1991.

[11] Stephen Boyd and John Doyle. Comparison of peak and RMS gains for discrete-time systems. *Systems & Control Letters*, 9(1):1–6, 1987.

[12] Stephen Boyd, Laurent El Ghaoui, Eric Feron, and Venkataramanan Balakrishnan. *Linear matrix inequalities in system and control theory*. SIAM, 1994.

[13] Herm Jan Brascamp and Elliott H Lieb. Best constants in Young's inequality, its converse, and its generalization to more than three functions. *Advances in Mathematics*, 20(2):151–173, 1976.

[14] Steven L Brunton and Bernd R Noack. Closed-loop turbulence control: Progress and challenges. *Applied Mechanics Reviews*, 67(5), 2015.

[15] VijaySekhar Chellaboina, Wassim M Haddad, Dennis S Bernstein, and David A Wilson. Induced convolution operator norms of linear dynamical systems. *Mathematics of Control, Signals and Systems*, 13:216–239, 2000.
[16] M.N Dao and Dominikus. Noll. Minimizing the memory of a system. *Mathematics of Control, Signals and Systems*, 27(1):77–110, 2015.
[17] J.C Doyle and Ch Ch Chu. Robust control of multivariable and large scale systems. Technical Report AD-A175 058, Honeywell Systems and Research center, 1986.
[18] Klaus-Jochen Engel, Rainer Nagel, and Simon Brendle. *One-parameter semigroups for linear evolution equations*, volume 194. Springer, 2000.
[19] B Francis and Keith Glover. Bounded peaking in the optimal linear regulator with cheap control. *IEEE Transactions on Automatic Control*, 23(4):608–617, 1978.
[20] Pascal Gahinet and Pierre Apkarian. A linear matrix inequality approach to H_∞ control. *International Journal of Robust and Nonlinear Control*, 4(4):421–448, 1994.
[21] D Hinrichsen and AJ Pritchard. On the transient behaviour of stable linear systems. In *Proc. 14th International Symposium of Mathematical Theory of Networks and Systems (MTNS 2000), Perpignan*, pages 19–23, 2000.
[22] D. Hinrichsen and A.J. Pritchard. On the transient behaviour of stable linear systems. *Proc. Int. Symp. Math. Theory Networks & Syst. Perpignan, France. CDROM - paper B218.*, 2:2, 2000.
[23] Simon J. Illingworth, Aimee S. Morgans, and Clarence W. Rowley. Feedback control of cavity flow oscillations using simple linear models. *Journal of Fluid Mechanics*, 709:223–248, 2012.
[24] Aniketh Kalur, Peter Seiler, and Maziar S Hemati. Nonlinear stability analysis of transitional flows using quadratic constraints. *Physical Review Fluids*, 6(4):044401, 2021.
[25] Hana Krakovská, Christian Kuehn, and Iacopo P. Longo. Resilience of dynamical systems. *European Journal of Applied Mathematics*, page 1–46, 2023.
[26] Heinz-Otto Kreiss. Über die Stabilitätsdefinition für Differenzengleichungen die partielle Differentialgleichungen approximieren. *BIT Numerical Mathematics*, 2:153–181, 1962.
[27] Colin Leclercq, Fabrice Demourant, Charles Poussot-Vassal, and Denis Sipp. Linear iterative method for closed-loop control of quasiperiodic flows. *Journal of Fluid Mechanics*, 868:26–65, 2019.
[28] Randall J LeVeque and Lloyd N Trefethen. On the resolvent condition in the Kreiss matrix theorem. *BIT Numerical Mathematics*, 24(4):584–591, 1984.
[29] Zongli Lin. Co-design of linear low-and-high gain feedback and high gain observer for suppression of effects of peaking on semi-global stabilization. *Automatica*, 137:110124, 2022.
[30] Chang Liu and Dennice F Gayme. Input-output inspired method for permissible perturbation amplitude of transitional wall-bounded shear flows. *Physical Review E*, 102(6):063108, 2020.
[31] Edward N Lorenz. Deterministic nonperiodic flow. *Journal of Atmospheric Sciences*, 20(2):130–141, 1963.
[32] F. Martinelli, M. Quadrio, J. McKernan, and J. F. Whidborne. Linear feedback control of transient energy growth and control performance limitations in subcritical plane poiseuille flow. *Phys. Fluids*, 23(1):014103, 2011.
[33] Robust control toolbox 6.11, 2021. The MathWorks, Natick, MA, USA.
[34] Tim Mitchell. Computing the Kreiss constant of a matrix. *SIAM Journal on Matrix Analysis and Applications*, 41(4):1944–1975, 2020.
[35] Tim Mitchell. Fast interpolation-based globality certificates for computing Kreiss constants and the distance to uncontrollability. *SIAM Journal on Matrix Analysis and Applications*, 42(2):578–607, 2021.
[36] Talha Mushtaq, Peter J Seiler, and Maziar Hemati. Feedback stabilization of incompressible flows using quadratic constraints. In *AIAA AVIATION 2022 Forum*, page 3773, 2022.
[37] Andy Packard, Kemin Zhou, Pradeep Pandey, and Greg Becker. A collection of robust control problems leading to LMIs. In *[1991] Proceedings of the 30th IEEE Conference on Decision and Control*, pages 1245–1250. IEEE, 1991.
[38] A. Papachristodoulou, J. Anderson, G. Valmorbida, S. Prajna, P. Seiler, P. A. Parrilo, M. M. Peet, and D. Jagt. *SOSTOOLS: Sum of squares optimization toolbox for MATLAB.* `http://arxiv.org/abs/1310.4716`, 2021. Available from `https://github.com/oxfordcontrol/SOSTOOLS`.
[39] Pierre Quénon and James F Whidborne. Control of plane poiseuille flow using the kreiss constant. In *International Conference Cyber-Physical Systems and Control*, pages 41–51. Springer, 2021.

[40] P. J. Schmid and L. Brandt. Analysis of fluid systems: Stability, receptivity, sensitivity. Lecture Notes from the flow-nordita summer school on advanced instability methods for complex flows, Stockholm, Sweden, 2013. *Applied Mechanics Reviews*, 66(2):024803, 2014.

[41] MN Spijker. On a conjecture by Leveque and Trefethen related to the Kreiss matrix theorem. *BIT Numerical Mathematics*, 31:551–555, 1991.

[42] Jos F Sturm. Using sedumi 1.02, a matlab toolbox for optimization over symmetric cones. *Optimization methods and software*, 11(1-4):625–653, 1999.

[43] HJ Sussmann and PV Kokotovic. The peaking phenomenon and the global stabilization of nonlinear systems. *IEEE Transactions on automatic control*, 36(4):424–440, 1991.

[44] D Swaroop and D Neimann. On the impulse response of LTI systems. In *Proceedings of the 2001 American Control Conference.(Cat. No. 01CH37148)*, volume 1, pages 523–528. IEEE, 2001.

[45] Lloyd N Trefethen and M Embree. *Spectra and pseudospectra, the behavior of nonnormal matrices and operators*. Princeton University Press, 2005.

[46] Lloyd N Trefethen, Anne E Trefethen, Satish C Reddy, and Tobin A Driscoll. Hydrodynamic stability without eigenvalues. *Science*, 261(5121):578–584, 1993.

[47] J. F. Whidborne and J. McKernan. On the minimization of maximum transient energy growth. *IEEE Transactions on Automatic Control*, 52(9):1762–1767, 2007.

[48] James F Whidborne, John McKernan, and Anthony J Steer. Minimization of maximum transient energy growth by output feedback. *IFAC Proceedings Volumes*, 38(1):283–288, 2005.

[49] James A Yorke. A theorem on Liapunov functions using $\ddot{V}$. *Mathematical Systems Theory*, 4(1):40–45, 1970.

[50] Jerzy Zabczyk. *Mathematical Control Theory: an introduction*. Birkhäuser, Boston, 2008.

[51] K. Zhou, J. C. Doyle, and K. Glover. *Robust and Optimal Control*. Prentice Hall, 1996.